PEOPLE'S DEMOCRATIC REPUBLIC OF ALGERIA

MINISTRY OF HIGHER EDUCATION AND SCIENTIFIC RESEARCH

ECHAHID CHEIKH LARBI TEBESSI UNIVERSITY OF TEBESSA

FACULTY OF EXACT SCIENCES AND THE SCIENCES OF NATURE
AND LIFE

DEPARTMENT OF MATTER SCIENCES

THESIS of MASTER

Specialty: **Physics of materials**

Effect of Cr doping on optical and electrical properties of ZnO thin films deposited by spray pyrolysis technique

Presented by:

Rahma BENMERAD

Members of jury:

Dr. Mourad KHECHBA	President	Univ. Tebessa
Dr. Labidi HERISSI	Supervisor	Univ. Tebessa
Dr. Radhia BOUKHALFA	Examiner	Univ. Tebessa

University season: 2022/2023

PEOPLE'S DEMOCRATIC REPUBLIC OF ALGERIA

MINISTRY OF HIGHER EDUCATION AND SCIENTIFIC RESEARCH

ECHAHID CHEIKH LARBI TEBESSI UNIVERSITY OF TEBESSA

FACULTY OF EXACT SCIENCES AND THE SCIENCES OF NATURE AND LIFE

DEPARTMENT OF MATTER SCIENCES

UNIVERSITY LARBI TEBESSI .TEBESSA

THESIS of MASTER

Specialty: **Physics of materials**

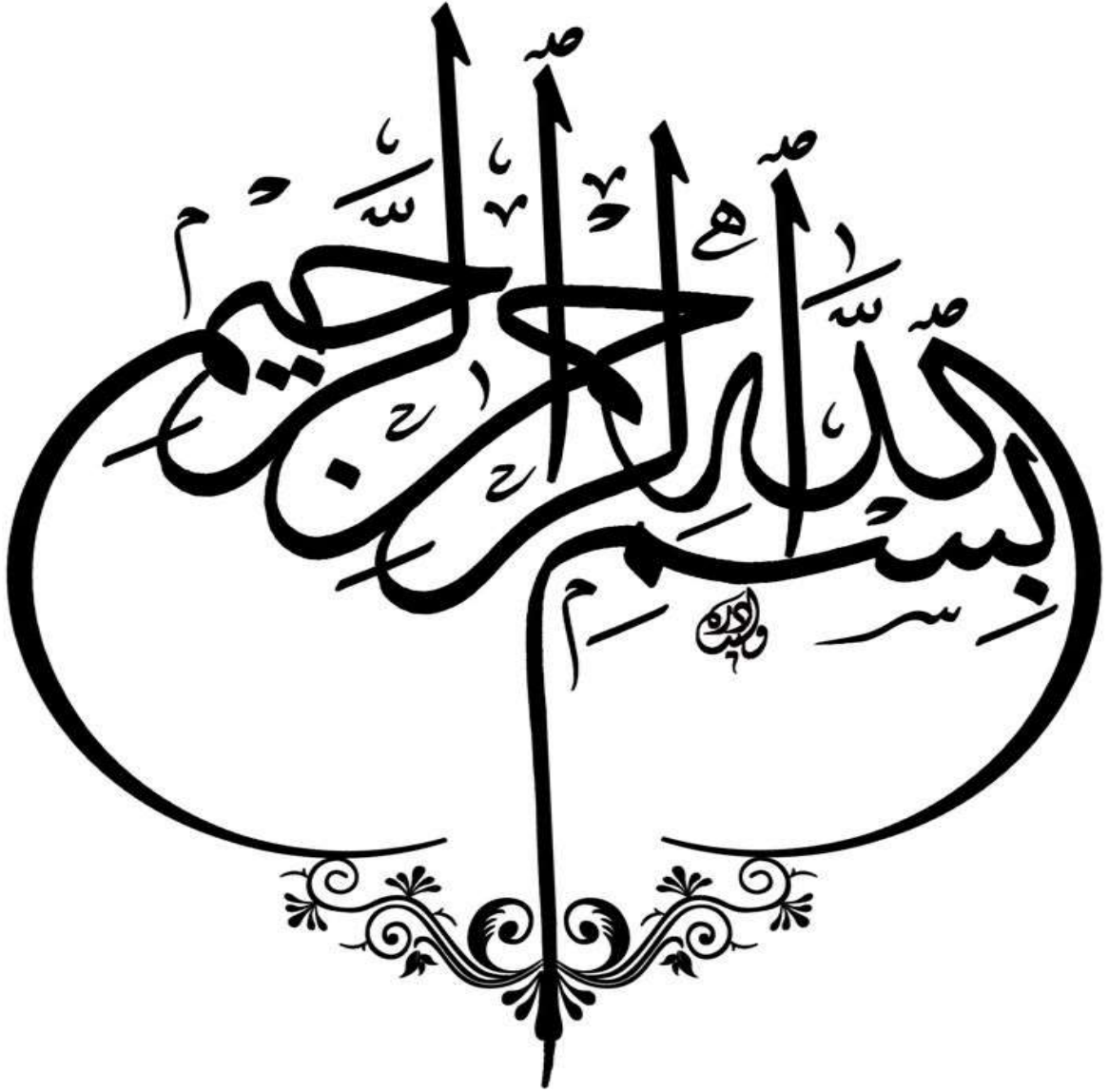# Effect of Cr doping on optical and electrical properties of ZnO thin films deposited by spray pyrolysis technique

Presented by:

Rahma BENMERAD

Members of jury:

Dr. Mourad KHECHBA	President	Univ. Tebessa
Dr. Labidi HERISSI	Supervisor	Univ. Tebessa
Dr. Radhia BOUKHALFA	Examiner	Univ. Tebessa

University season: 2022/2023

«يَرْفَعِ اللَّهُ الَّذِينَ آمَنُوا مِنكُمْ وَالَّذِينَ أُوتُوا الْعِلْمَ دَرَجَاتٍ»

المجادلة – الآية 11

Dedication

I dedicate this graduation to the one who drank the cup empty to give me a drop of love, to the one who reaped the thorns on my path to pave the pave of khowledge, *my mother and my father*

I dedicate my graduation to the one whose supplication was the secret of my success and her tenderness as a balm for my wounds, to the dearest of my beloved ones, my beloved *mother*, my support, my strength and my refuge after God, to the one who made heaven under her feet, to the one who flooded me with the flood of her tenderness, to the one who burned me in order to illuminate my path.

To my *affectionate mother, my sister, and my friend*, my God bless you with a crown above my head.

I dedicate this work to my great, amazing and wonderful, the father who learned me how I don't give up, no matter the circumstances, no matter how hard the life is, and how I should always move towards my goal and to work hard to achieve it. He has always been my true supporter at all times, *my father* who has forgotten how to live so that we may live, who spent his entire life for me. With out him, I would not have been able to follow my path.

my dear *father*, you are the most wonderful flower that I picked from this life. I will make you always proud of me. I wish God protect you for me.

I dedicate this graduation to those who showed me what is more beautiful than life, to those whose love runs through my veins, to whom I owe a lot to my brothers *Abderrahman*, *Ahmed Taha* and my sisters *Raoudha* and *Hiba Wissem*. I wish God bless you all for me.

Finally, I dedicate this graduation to my dear grandmother's (*Tita*) soul God have mercy on her.

Table of contents

TABLE OF CONTENTS

Table of contents

Chapter II: Elaboration and characterization of Cr-doped ZnO thin films

Part one : Elaboration of Cr-doped ZnO thin films………………………............

Part two: Characterization techniques of thin films…………………………...

Table of contents

Chapter III: Results and discussion

List of figures

List of figures

List of tables

List of tables

List of symbols

Symbol	Signification	Unit
M	Mass molar	g/mol
C	Solution concentration	mol/l
m	Mass	g
V	Volume	l
T	Temperature	^{o}C
α	Absorption coefficient	cm^{-1}
n	Refractive index	
E_g	Energy of optical band gap	eV
T	Optical transmittance	%
I	Intensity of light	cd
t	Film thickness	nm
λ	Wavelength of incident photon	nm
φ_S	Spray flow rate	ml/h
$h\upsilon$	Energy of incident photon	eV
E_{Urb}	Urbach energy	meV
I	Electrical current	A
V	Voltage	V
ρ_s	Surface resistivity	Ω/sqr
σ	Electrical conductivity	$\Omega^{-1}.cm^{-1}$
$d_{N\text{-}S}$	Nozzle-substrate distance	cm

List of abbreviation

ZnO	Zinc oxide
CrO	Chromium oxide
CrO_2	Chromium dioxide
Cr_2O_3	Dichromium trioxide
$CrCH$	Chromium chloride hexahydrate
$ZnO{:}Cr$	Chromium doped zinc oxide
PLD	Pulsed-laser deposition
DC	direct current
RF	radio frequency
CVD	Chemical vapor deposition
CSD	Chemical solution deposition
$PECVD$	Plasma Enhanced Chemical Vapor Deposition
$MOCVD$	Metal-Organic Chemical Vapor Deposition
$LPCVD$	Low Pressure Chemical Vapor Deposition
$Sol-Gel$	Solution–Gelling
$TCOs$	transparent conducting oxides
ZAD	Zinc acetate dihydrate
$UV-Vis-NIR$	Ultraviolet-visible-near infrared

General introduction

Hello. My name is Stephen Hawking - physicist, cosmologist and something of a dreamer. Although I cannot move and I have to speak through a computer, in my mind, **I am free.**
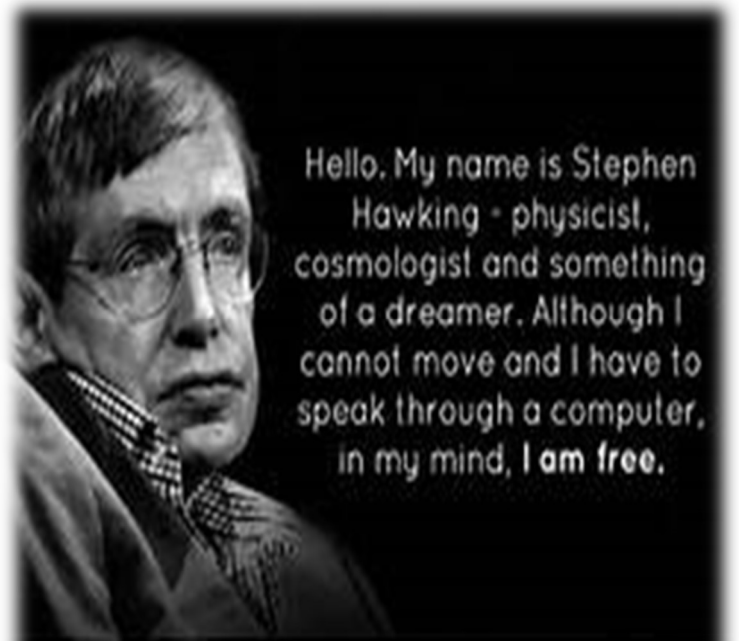
General introduction

In recent years, great efforts have been made in the field of developing thin films of transparent conductive oxides (TCOs) [1]. They constitute a unique class of materials, which combine two physical properties together: high optical transparency and high electrical conductivity. TCOs like ZnO and Cr_2O_3 films have attracted the attention of many research workers due to their wide range of applications such as solar cells and gas sensors [2].

Metal oxides are generally wide gap semiconductors, they divide into two large families, the first concerns the n-types (conduction by electrons) and the second family includes the p- types (conduction by holes). They are known because they are environmentally friendly, exist in abundance in the earth, easy to synthesize and less expensive [3]. They are known to be relatively unstable because of their tendency to exchange oxygen from their network easily with air [4].

Zinc oxide (zinc white or zinc flower) is known as zincite, it is an n-type semiconductor, transparent in the visible whose refractive index in bulk form is equal to 2 and has a large direct optical gap (3.3 eV) and a large exciton binding energy (60 meV), their electrical conductivity is very high $(10^{-6} - 10^{2}(\Omega.cm)^{-1})$. The stable phase of ZnO is the compact hexagonal structure of würtzite type (hc), their lattice parameters are a = b = 3.2499 Å and c = 5.206 Å [5,6]. Zinc oxide has interesting electronic, electrical and optical properties for optoelectronic applications, particularly in the photovoltaic field [7,8].

Chromium oxide is an inorganic compound and it has many structures such as: CrO, CrO_2 but the most famous and useful one is Cr_2O_3 [9]. It is found in nature in the form of a rare mineral known as Escolaite, where it is considered one of the most important chromium oxides, due to its distinction in several properties including: Cr_2O_3 comes in the form of a green powder and is a p-type semiconductor with a direct bandgap (3 eV) [9-11]. In fact, chromium oxide can be used in metallurgy in making refractory bricks, so it is added to annealed glass or as a magnetic pigment in magnetic video and audio tapes to store information. Cr_2O_3 is also used as a polishing agent for various purposes such as gemstones, diamonds, glass and eye glasses [12]. Though undoped zinc oxide and chromium-doped zinc oxide thin films may be prepared by various techniques, such as: sputtering, electron beam evaporation, sol–gel, chemical vapor deposition, and spray pyrolysis. The methods that are used more often for depositing oxide thin films were spray pyrolysis being one of the most cost-effective methods due to its ability to

deposit large uniform area with low fabrication cost, simplicity and low deposition temperature [2,13,14].

The objective of this work is the elaboration of undoped and Cr-doped ZnO thin films onto glass substrates heated at 400°C, by ultrasonic spray pyrolysis technique, from precursor solution of zinc acetate dihydrate ($Zn(C_2H_3O_2)_2 \cdot 2H_2O$) and chromium chloride hexhydrate ($CrCl_3 \cdot 6H_2O$) at two different nozzle- substrate distances, and the study of the effect of Cr-doping percentage and nozzle-substrate distance on the properties of ZnO thin films. The deposit was made at the level of laboratory of material and structure of electromechanically systems and their reliability (LMSSEF) of Larbi Ben M'hidi University of Oum El Bouaghi. These films are characterized by UV-Visible-NIR double beam spectrophotometer and four-point probe technique to determine their optical and electrical properties, respectively.

Our work is divided into three chapters as follows:

- In the first chapter, we present overview on thin film, the definition of metal oxides, the essential properties of zinc oxide and chromium oxide (structural, optical, and electrical) and the field of their applications. Also, we mentioned the deferent deposition techniques which used to develop TCOs thin films, such as spray pyrolysis, which is very attractive for making functionally graded thin films.

- The second chapter is devoted to the elaboration of undoped zinc oxide and Cr-doped ZnO thin films.

- In the third chapter, we present the discussions of the experimental results obtained of undoped and Cr-doped zinc oxide thin films.

In the last, we conclude our work with general conclusion that summarizes the different steps and results achieved in this work.
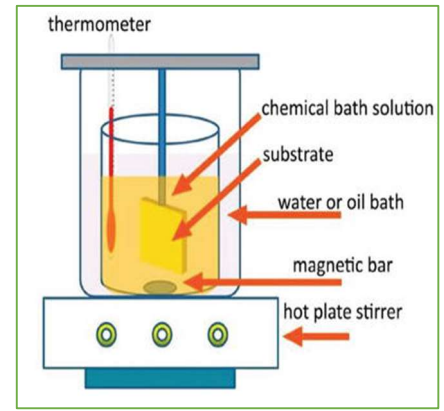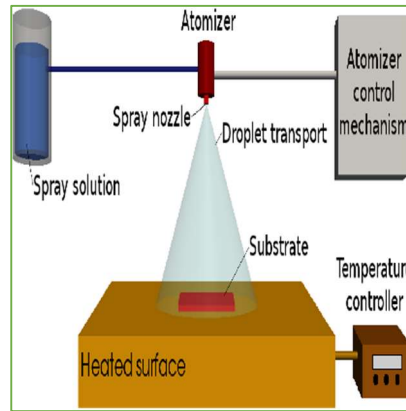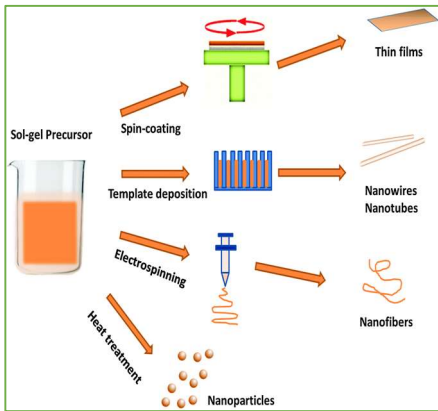
Chapter I

Bibliographic studies of zinc oxide and chromium oxide thin films
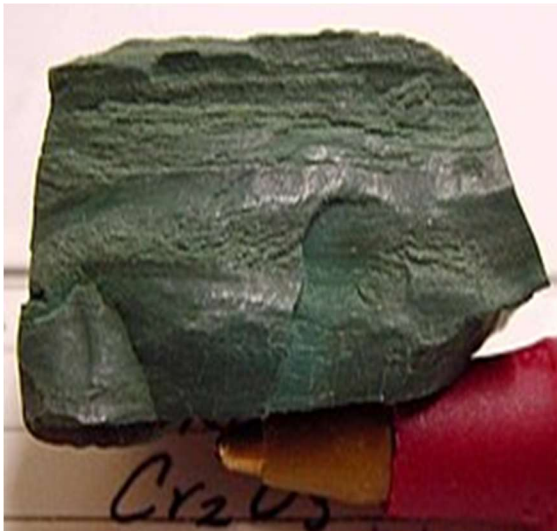
Chapter I: Bibliographic studies of ZnO and Cr_2O_3 thin films

I.1. Overview on thin film

The thin films of metal oxides are remarkable materials in the last years since they have several fields of industrial applications. Among these oxides, zinc oxide. This chapter is devoted to the bibliographical study on thin film and their deposition methods. According to the deposition processes detailing the general properties of zinc oxide citing its structural, optical, electrical properties and their applications.

I.1.1. Thin film concept

In principle, a thin film of a given material is an element of this material of which one of the dimensions called the thickness has been greatly reduced in such a way that this small distance between the two limiting surfaces remains order of the μm, which gives the layer the quasi-two-dimensionality, which leads to a disturbance of the majority of the physical properties. The essential difference between the material in the bulk state and that in thin films is related to the fact that in the bulk state one generally neglects with reason the role of the limits in the properties, while in a thin films it is on the contrary the effects related to boundary surfaces, which are preponderant. It is quite obvious that the lower the thickness, the greater this two-dimensional effect, and that conversely, when the thickness of a thin film exceeds a certain threshold, the effect of minimal thickness and the material will regain the properties well known from bulk material [15].

I.1.2. Thin film applications

The implementation of thin film manufacturing technologies has led to many applications in very diverse fields which it shown in Figure I.1.
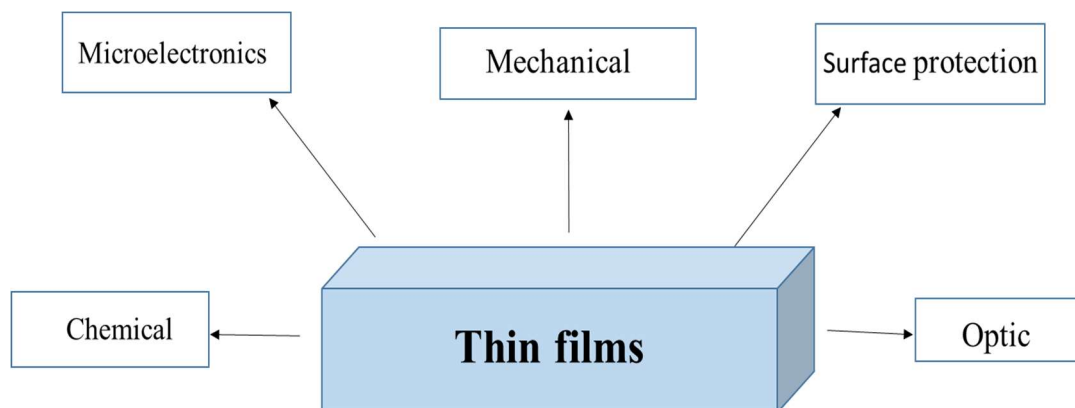
Figure I.1. Thin film applications [16].

Modifying the surface of a substrate makes it possible to couple the properties of the core material (or substrate) and of the surface material: the latter can be either directly derived from the substrate in the case of a surface treatment or a filler material for a surface coating. The first surface modifications had an aesthetic purpose (painting, gold plating, enamelling, etc.), while more technical applications concerned metallurgy (cementation, nitriding,…etc). During the 20th century, more advanced applications have diversified into the following areas [5,6,16,17]:

- **Microelectronics:** PN junction, Transistor, Piezoelectric material, LED lamp, Superconductor, etc.

- **Optics:** Anti-reflective layers in solar cells, Mirror staining, Anti-reflective treatment of camera lenses, Photo detection, Flat screen displays, Ophthalmic applications, Optical guides, etc.

- **Mechanical:** Dry lubrication; Resistance to wear, Diffusion barriers, etc.

- **Chemistry:** Waterproof film (corrosion resistance), Gas sensor, Catalytic coatings, protective films, etc.

- **Thermal:** Thermal barrier layer.

- **Micro and nanotechnologies**: Mechanical and chemical sensors, Micro fluidics, Actuators, Adaptive optics, Nano photonics, etc.

- **Magnetic**: Information storage (computer memory), Security devices, Magnetic sensors, etc.

- **Decoration:** Watches, Glasses, Jewellery, Household equipment, etc.

I.1.3. Mechanism of thin films formation

The formation of thin films is one of the aspects of such development where the restriction as dimensional growth rules out the existence of two-dimensional thin films. This has vast range of applications in different areas. Thin films can be prepared from variety of materials such as metals, semiconductors, insulators or dielectric. For the deposition of thin films various preparation methods have been developed as well as new methods are also being evolved to improve the quality of thin films deposit with maximum reproducible properties and minimum variation in their compositions. In the thin film deposition process, following basic steps are to be considered [15,18,19]:

- The initial materials used for the deposition is prepared in the atomic, molecular or finest particulate form before the deposition,

- The finest form of materials is transported on the substrate in the form of vapor stream, the solid, or the spray,

- Deposition of the material on the substrate and the film growth by nucleation-growth process.

I.1.4. Classification of thin film deposition techniques

The process of thin film deposition occurs by multiple techniques with its requirement of being single or multicomponent, alloy/oxide/compound coating on substrate of different shapes and size (Figure I.2). Depending on the nature of way used for the thin films, deposition the technique can be broadly classified as [2]:

- Physical deposition techniques,

- Chemical deposition techniques.

Thin Film Deposition Techniques

Physical Deposition Techniques (P.D)

Chemical Deposition Techniques (C.D)

Sputtering

Vacuum evaporation

In solution phase (CSD)

In vapor phase (CVD)

-D.C
-R.F
-Magnetron

-Joule heating
-Laser ablation (PLD)
-Electron beam heating

-Sol-gel
-Electrodeposition
-Spray pyrolysis

-ALCVD
-PECVD
-MOCVD
-APCVD
-LPCVD
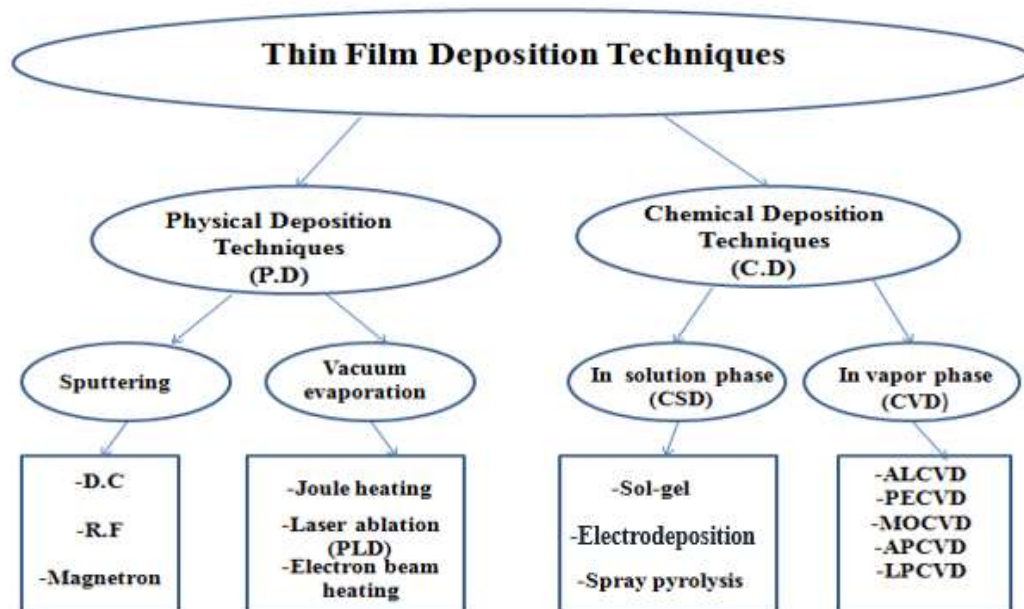
Figure I.2. Diagram of the different techniques of thin film deposition.

I.1.4.1. Physical deposition techniques

The physical deposition techniques are those in which the material required for deposition is made available in the atomic, molecular or particulate form before deposition. This is usually done at sufficiently high temperature. The condensation of vapor on substrate material kept at relatively low temperature yields. Physical deposition can be further subdivided in: Vacuum evaporation and Sputtering [13].

I.1.4.1.1. Vacuum evaporation

Vacuum evaporation technique is the simplest technique used to prepare amorphous thin films especially chalcogenide and oxide films such as CdSSe, MnS, Ge-Te-Ga, ZnO & Cr$_2$O$_3$ [20,21].

The evaporation of a material to be deposited is obtained by heating it by one of the different means: Joule effect, induction (coupling of a high frequency generator), electron gunlaser beam or electric arc [22,23]. In addition the literature shows that this process is as well suitable for the production of ZnO films. Indeed, different thin films of undoped and doped ZnO, have been successfully prepared by vacuum evaporation [17].

a) Joule heating

The simplest forms of evaporation sources are wires and sheets of refractory materials (Mo, Ta and W). As the electrical resistances of these sources are low, they must be heated from a low voltage, high current power supply (Figure I.3) (e.g. 0-5 V and 0-400 A or 2 kW alternating current) [6,17]. The ZnO layer can be obtained by thermal evaporation from powdered zinc oxide after annealing in an air atmosphere [15].
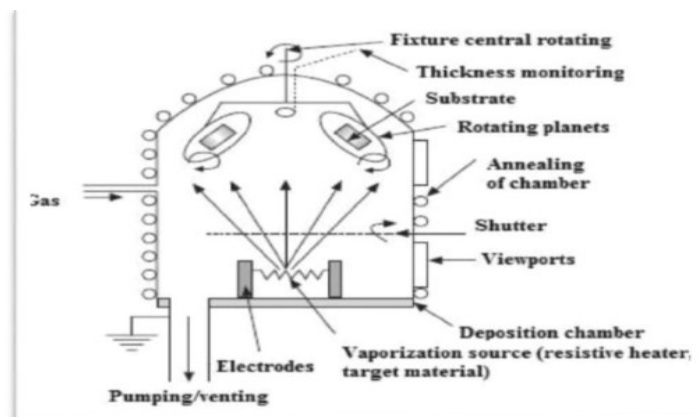
Figure I.3. Schematic of vacuum thermal evaporation technique [2].

b) Laser ablation

Laser ablation or Pulsed Laser Deposition (PLD) is another physical deposition technique to deposit the thin film-coating system [7]. PLD depends on focusing a laser beam on a material in order to vaporize it and then condense the ionized particles on a substrate heated or not. It should be noted that the ionized particles have a high kinetic energy (a few tens of electron volts). Figure I.4 shows the schematic diagram of PLD [24].

Different kinds of laser sources are being used to ablate the target, the most common sources are KrF (248 nm), XeCl (308 nm), and Nd-YAG laser (1064 nm). In the case deposition of thin layers of ZnO by PLD has the advantage of being able to use of high oxygen and that of making high quality crystalline films with speed of high growth even at low temperature [7,25,26].
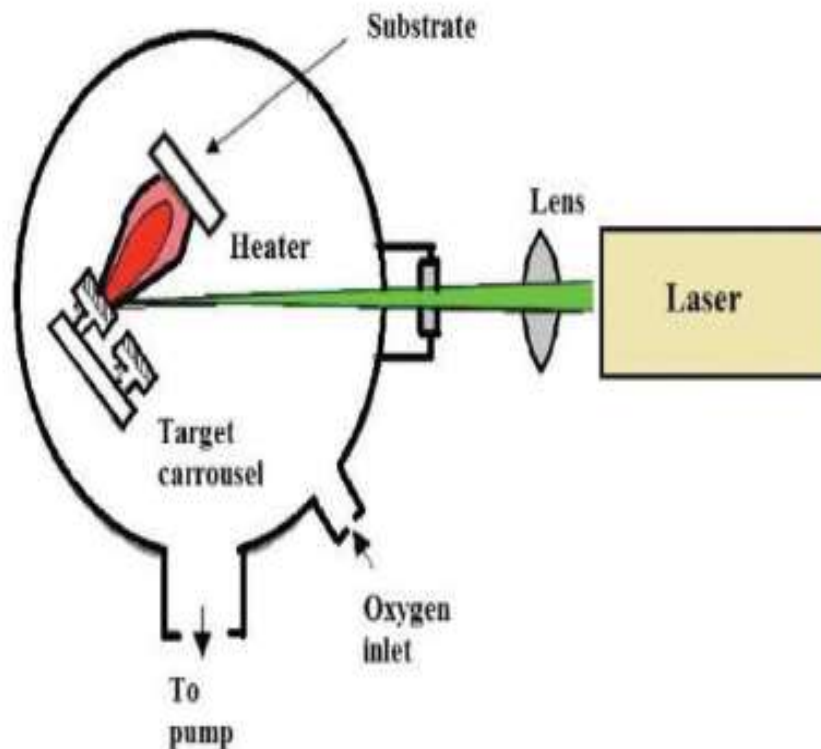
Figure I.4. Schematic of pulsed-laser deposition [27].

c) Electron beam heating

The principle of this method is presented in Figure I.5. The electron beam generated by a tungsten filament (W) is deflected by an electromagnet towards the crucible containing the material. This technique has two important advantages [2,6,13]:

❖ It is easy to control the applied power, therefore the evaporation rate. Consequently, the deposition on the substrates can be easily controlled in a wide range of speeds, from very low to very important,

❖ The material to be evaporated is placed in a water-cooled copper crucible, which eliminates the problems due to contaminations by the crucible.
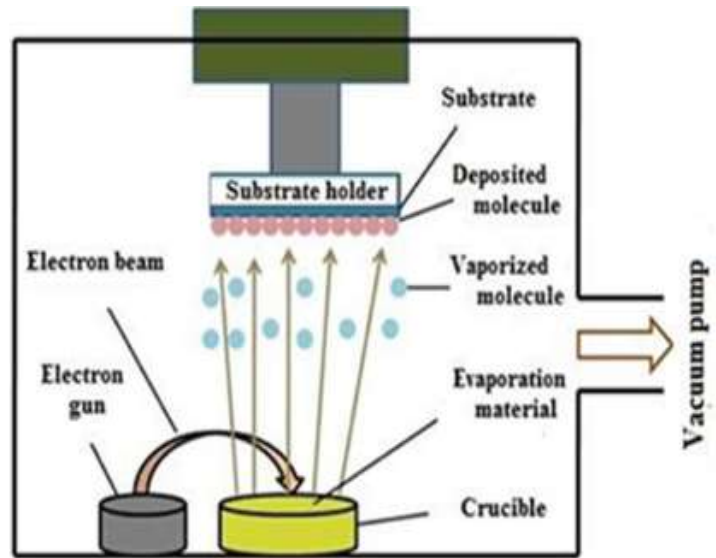
Figure I.5. Schematic diagram of electron beam evaporation [1].

I.1.4.1.2. Sputtering

In this method, the substrate is placed in a container containing a gas (generally argon) at low pressure in which an electric discharge occurs. This discharge has a role in ionizing gas atoms. The ions obtained are accelerated by the voltage difference and bombardment of the cathode formed by the material to be deposited (the target) under the action of the accelerated ions, and the atoms are torn off from the cathode and deposited on the substrate [2,22,28]. Figure I.6 shows the diagram of the sputtering process [13].
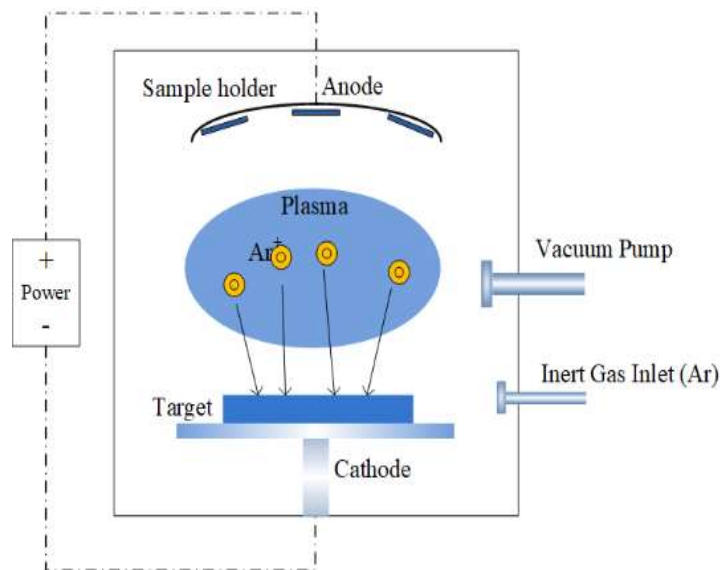
Figure I.6. Schematic of the sputtering process [13].

There are three common types of sputtering process [3,26,29,30]: direct current (DC), radio frequency (RF) and magnetron sputtering.

-The first one, depends on DC power, which is generally used with electrically conductive target materials. It is easy to control with low-cost option.

-The second one, sputtering uses RF power for most dielectric materials.

-The third one magnetron process, for which permanent magnets distributed around the chamber make it possible to create a magnetic confinement of the plasma and thereby to increase the ionization efficiency of the electrons which then carry out helical trajectories.

I.1.4.2. Chemical deposition techniques
I.1.4.2.1. Chemical deposition in vapor phase

Chemical vapor deposition (CVD) is a versatile technique used to deposit gas phase reactants (precursors) onto a solid substrate forming thin films. CVD can be used to deposit large areas such as microelectronics. This technique is capable of depositing highly dense and pure films in addition to having good adhesion uniformity. CVD also has the ability to control crystal structure and film formation by varying the substrate temperature and deposition rate. However, it has many drawbacks: high substrate temperature, low density coating, impure deposits, expensive equipment and dangerous gases [31]. There are several types of CVD technologies, including [6,17,25,26,31]:

a) **The PECVD**: Plasma-enhanced chemical vapor deposition (Figure I.7). This is a method that allows the production of a solid precipitate from a gaseous substance and a chemical reaction with the help of an electric discharge then follows a chemical reaction.
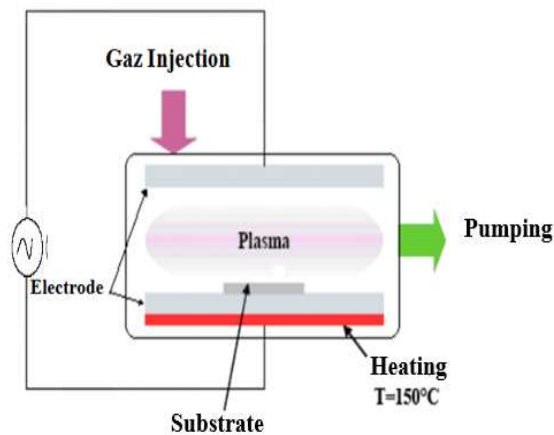
Figure I.7. PECVD system diagram [6,17].

b) **The MOCVD**: Metal Organic Chemical Vapor Deposition at atmospheric pressure or low pressure.

c) **The APCVD:** Atmospheric Pressure Chemical Vapor Deposition.

d) **The LPCVD:** Low-pressure chemical vapor deposition as opposed to APCVD (Atmospheric Pressure CVD), depending on whether one operates under reduced pressure or at atmospheric pressure.

e) **The ALCVD:** Atomic Layer Chemical Vapor Deposition.

I.1.4.2.2. Chemical deposition in solution phase

The chemical solution deposition (CSD) is a technique as a highly flexible method for the fabrication of electronic oxide thin films is reviewed. The main interest of chemical deposition in solution is its simplicity and its ease of controlling the deposition conditions of elaboration. The realization of thin films of ZnO by this method is done according to three steps: preparation of the solution, cleaning of the substrates and deposition on the substrate. There are several variants of solution deposition such as: sol-gel, electrodeposition and spray pyrolysis [5,26].

a) **Sol-gel process**

Sol-gel process is used for production of solid materials from small molecules. Oxides of silicon and titanium are the most popular materials for this process [1]. The basic principle of the Sol-Gel process is as follows: a solution based on precursors in the liquid phase is transformed into a solid by a set of chemical reactions (hydrolysis-condensation reactions) of the polymerization type at a temperature close to environment [5,13,32]. Dip-coating and spin-coating techniques are the best known and most used techniques [33]:

1/ Spin coating: Spin coating process consists of putting the drops of liquid precursor on the surface of a spinning substrate (Figure I.8). The film formed on the substrate results from two balancing forces:

The centrifugal force (due to spinning) which drives the viscous sol radially outwards and viscous force (due to friction) which acts radially inwards.

Spin coating is the cheapest film production method in silicon technology. However, thinner films (<100 nm) are hard to make and can waste 98% of the process materials [1].
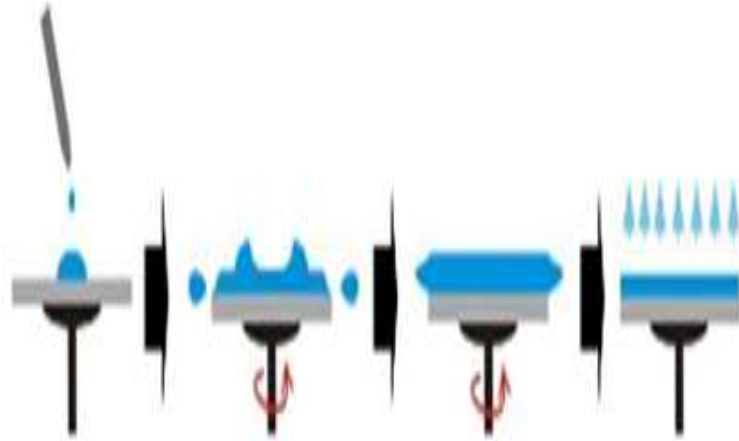
Figure I.8. Spin coating process diagram [7].

2/ Dip coating: In this method (Figure I.9), the substrate is normally withdrawn vertically from a desired coating solution, which causes a complex process involving gravitational draining with concurrent drying and continued condensation reactions [1].
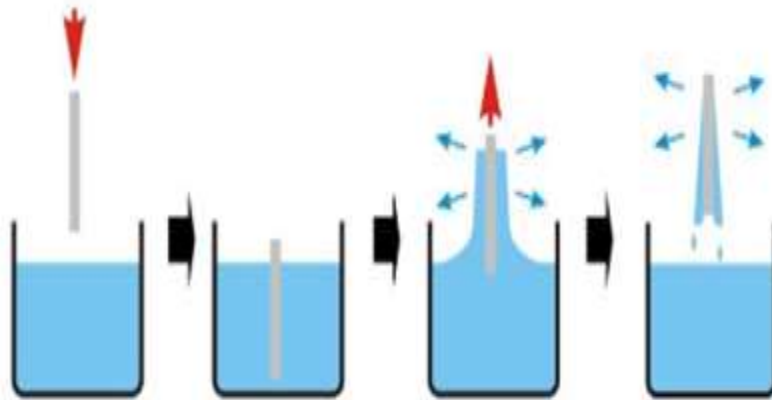
Figure I.9. Dip-coating process diagram [7].

b. Electrodeposition process

Electrodeposition is a non-vacuum electrochemical technique preferable for thin film deposition owing to its ability to deposit multicomponent alloys at low temperature. In this method, the deposition of thin metallic films is done onto the substrate by the reduction of cations without any unwanted reactions [1]. The Figure I.10 shows the thin films electrodeposition process [1].
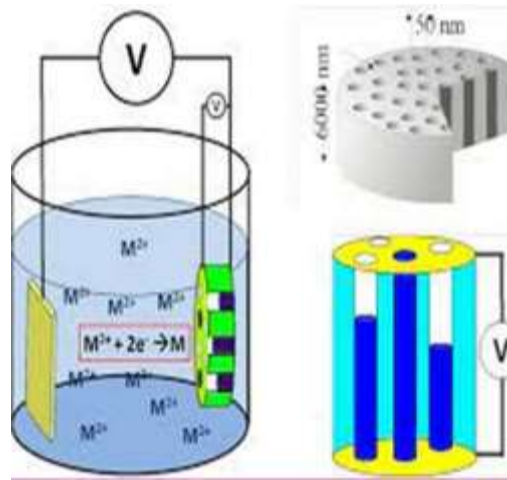
Figure I.10. Electrodeposition process to deposit thin films [1].

c. Spray-pyrolysis technique

The « spray » technique was first proposed by Chamberlin and Skarman in 1963. It was used successfully for the deposition of CdS films [17]. It was then adapted for the production of several materials such as (Cd, Zn) Sn, $CuInS_2$, FeS_2… as well as for obtaining thin films of transparent and conductive oxides (SnO_2, ZnO, NiO…) [25]. The "Spray pyrolysis" is the more common name for this technology. It consists of "atomization" and "pyrolysis" [7]. This method is based on spraying a solution containing the atoms to be precipitated, generally acetates, chlorides or nitrates that are easily soluble in water or alcohol to be deposited on a heated substrate [6,25]. Figure I.11 shows the diagram of spray pyrolysis deposition equipment.
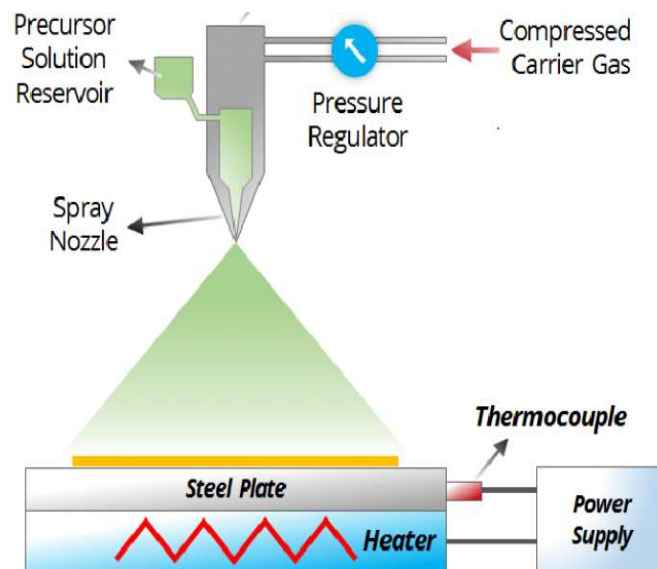
Figure I.11. Diagram of spray pyrolysis deposition equipment [25].

This method has many advantages [17,25]:

➢ Simple method of providing the precursor by means of a spray,

➢ Ease of construction of reactors of this type,

➢ Possibility of depositing a wide choice of materials,

➢ Simply controllable reaction environment, under neutral gas or under air at atmospheric pressure,

➢ The composition during deposition can be controlled, as it is possible to achieve layers of uniform thicknesses and compositions,

➢ Several products can be used at the same time, in particular for doping,

➢ The thin films prepared by this technique are of high and good quality,

➢ Excellent adhesion,

➢ It is a very inexpensive and economical technique,

➢ It is industrializable,

➢ Deposits can be made on large surfaces in the case of solar cells or flat screens,

➢ It does not require a pumping group like almost all the methods of thin films deposition.

These are all the advantages that motivated us to select this production process to carry out our work. In this technique, several parameters come into play, such as the nature of the precursor, the nature of the solvent, the concentration of the solution, the nature of the substrate, the deposition temperature, the nozzle-substrate distance, the spray flow rate, ….etc [25].

I.1.5. The choice of thin film deposition technique

In general, whatever the techniques for producing thin oxide films, the properties of the films produced are influenced by the following parameters [17]:

➢ The surrounding environment (gas, liquid, etc).

➢ The reagents used (nature, concentration, etc).

➢ The substrate (nature, temperature, etc).

➢ Any annealing of the films.

The choice of a thin film deposition technique depends on several factors [4,15,17] :

➢ The material to be deposited,

➢ The desired deposition rate,

➢ The limits imposed by the substrate, such as the maximum temperature of deposition,

➢ Adhesion of the deposit to the substrate,

➢ Deposition on substrates of complex shape or not,

➢ The purity of the material considered for the ideal solution, and for alternative solution,

➢ Ecological considerations,

➢ The ease of supply of the material to be deposited, in the present and in the future.

I.2. Metal oxides

Metal oxides (MO) are homogeneous solid phases containing one or more types of metal cations of different oxidation states ($M1_xM2_yO_z$), where M is the chemical symbol of the Metal atom considered, O the symbol of the oxygen atom, "x" and "y" and "z" natural integers, among the important metal oxide: Al_2O_3, ZnO, Cr_2O_3, CuO, Fe_2O_3, SnO_2, and $BaTiO_3$ [5,34]. The cations combine with the O^{-2} (oxide ions) to give well-defined crystallographic structures. Generally, to obtain the metal oxide, the oxygen is added to a metallic element (oxidation reaction). The methods of preparation, the chemical nature of the cations as well as the chemical composition of these oxides are of fundamental importance [35]. These cations lead to the variation of physical properties such as optical transmittance, electrical conductivity and specific surface area, thus inducing significant changes in the electrochemical and catalytic behavior of these materials. The oxide group is therefore one of the most varied classes of minerals in physical and chemical properties [15].

I.2.1. Classification of metal oxides

Metal oxides are classified according to: either the nature of the conduction (electrons or holes) or according to whether the metal oxides are simple or complex [15].

A) n-type and p-type metal oxides

There are two main families of metal oxides (Table I.1). The first concerns the p-types (conduction by holes), they are known to be relatively unstable because of their tendency to exchange oxygen from their network easily with the air. However, p-types are used for certain applications such as high temperature oxygen sensors [36].

Table I.1. Classification of metal oxides [18].

n-type Metal oxide	p-type Metal oxide
SnO_2	NiO
WO_3	PdO
ZnO	La_2O_3
TiO_2	Ag_2O
In_2O_3	TeO_2
Ta_2O_5	$BaTiO_3$

The second family includes the n-types (conduction by electrons), they fulfill the majority of gas sensor type applications because they are more stable and have more favorable properties for chemisorption [5,6]. Metal oxide semiconductors have been found useful for a variety of applications including catalysts, sensors, solar cells, diodes, and transistors [5,6].

B) Simple oxides and mixed oxides

Metal oxides can be classified into two main categories: simple metal oxides consist of a metal such as: SnO_2, TiO_2, SiO_2, …[6], and mixed oxides containing two or more components such as $BaTiO_3$ that have slightly or very different properties corresponding simple oxides. A particularly interesting property is the production of very acidic sites linked to the interface or to the bond between the two components [36].

I.3. Metal oxide doping

To improve electrical properties such as charge carrier concentration and electrical conductivity that are modified by doping. Depending on the material or type of doping, the doping can be substitution, vacation or implantation interstitial [4].

Doping causes new electron acceptor and donor levels to appear in the band structure of the doped material. These levels appear in the gap between the conduction band and the valence band. There are two different type of doping [37].

- **n-type doping:** During n doping, the introduction of electron donor atoms leads to the appearance of a pseudo energy level located just below the conduction band (Figure I.12.a). Thus, the energy necessary for the electrons to pass into the conduction band is much more easily achieved than in an intrinsic semiconductor [37]. In which their purpose is to produce an excess of carrier electrons in the semiconductor. This type of doping is done by replacing the atoms of the metal or oxygen [4,38,39].

- **p-type doping:** During p doping, the introduction of electron acceptor atoms similarly leads to the appearance of pseudo level located above valence band. The energy to be supplied to the valence electrons to pass on this acceptor level is low, and the departure of the electrons leads to the appearance of holes in the valence band [37,40]. In which their purpose is to create excess holes as shown in Figure I.12.b [4].

(a)   **(b)**
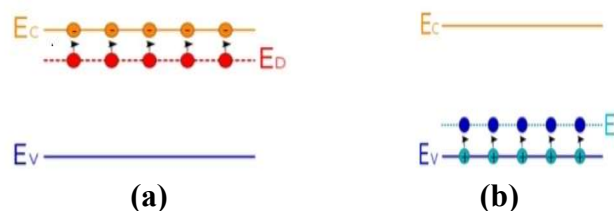
Figure I.12. Representation of the energy level of the doping element **(a)** n-type, **(b)** p-type [37].

I.4. Transparent conductive oxides

The discovery of oxides which are transparent with high electrical conductivity (TCO: Transparent Conductive Oxide) dates back to the beginning of the 20th century, when Bädeker found that the thin films of cadmium oxide (CdO) obtained by sputtering from thermal oxidation of cadmium films have the properties of optical transparency and electrical conduction [41]. This observation gave rise to a new research theme which remains a topical subject after a century. Many TCO materials then appeared such as: In_2O_3, In_2O_3:Sn, In_2O_3:F, SnO_2, SnO_2:Sb, SnO_2:Cd, SnO_2:F, ZnO, O:Al, Cd_2SnO_4, $CdSnO_2$, and also NiO [6,35,42,43].
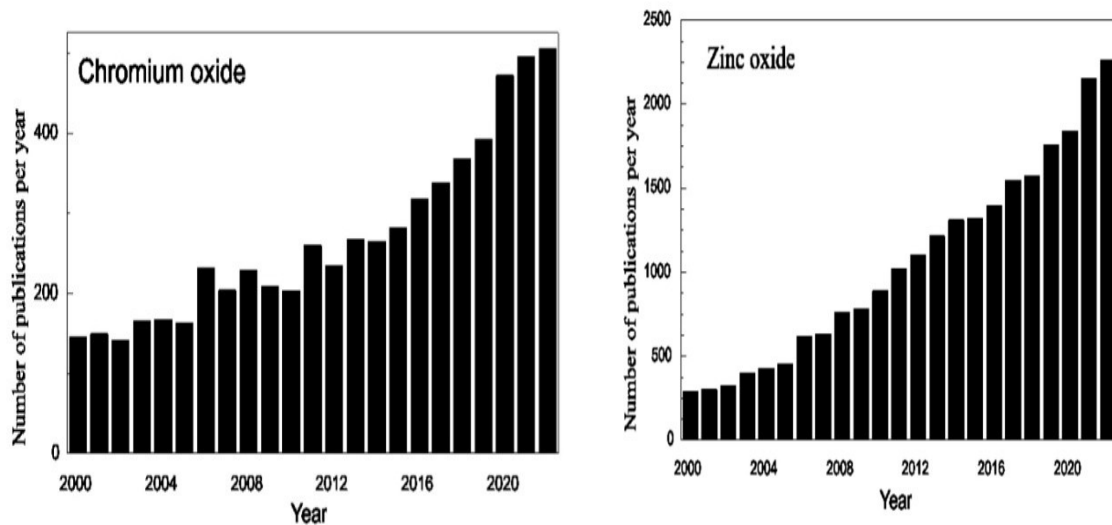
Figure I.13. Number of publications with the keyword: **(a).** "Cr_2O_3 or chromium oxide" and **(b).** "ZnO or Zinc oxide" in their title on the science direct website page from 2000 to 2022.

The diversity of TCOs and their applications corresponds to the fact that the criterion for choosing a TCO does not depend solely on the quality factor Q. But, for each material, other parameters are used in the corresponding field, such as thermal stability, chemical and mechanical, or again the toxicity, the low cost of preparation, the constraints of implementation, or also the output work (fundamental with regard to the injection of carriers). All these parameters play a key role in the choice of TCO.

Among the TCO, we are interested in ZnO and Cr_2O_3 because they have many applications in everyday objects. Figure I.13 shows respectively the evolution of the number of publications containing the keywords "ZnO or Zinc oxide" and "Cr_2O_3 or chromium oxide" in their title in the scientific publications of "science direct" (www.sciencedirect.com). These materials have a number of properties that will be detailed in this chapter.

I.5. Properties and applications of zinc oxide and chromium oxide

I.5.1. Zinc oxide properties

Zinc oxide (ZnO) is a well-known semiconductor that has wide direct band-gap (3.3 eV) at room temperature and large free excitation binding energy (60 meV). ZnO has high thermal stability, highly crystalline hexagonal structure, and high mechanical strength, which make it suitable for use as an electronic material in various fields such as bio-molecule sensor, ultraviolet light-emitting diode UV-LEDs, gas sensor, solar cell and optoelectronic [5,44].

The physico-chemical properties of zinc oxide make it a very interesting material for applications in optoelectronics and microelectronics. In what follows we present the main ones of these properties: structural, optical, and electrical.

I.5.1.1. Structural properties of ZnO

Zinc oxide (ZnO), known as Zincite in its natural state (Figure I.14) [17], can exist either as a powder or as a massive crystal. In table I.2, some general properties of ZnO are given.

Figure I.14. Photograph of a natural crystal of Zincite [45].

Table I.2. Some properties of ZnO [17].

General description	Density (g/cm^3)	Molecular density (molecules/cm^3)	Melting point (°C)	Enthalpyof formation (kcal/mol)	Solubility in H_2O at 29°C (g/l)
Colorless crystals, white powder	5.60	4.21×10^{22}	1975	83.17	0.0016

Depending on the production conditions, ZnO comes in three crystalline forms (Figure I.15): **i)** the würtzite type structure (hexagonal) which is stable under normal conditions, **ii)** Thesphalerite structure (CFC) which is unstable and which appears under high pressures, **iii)** the Rock–Salt (NaCl) structure which appears under very high pressures [17].
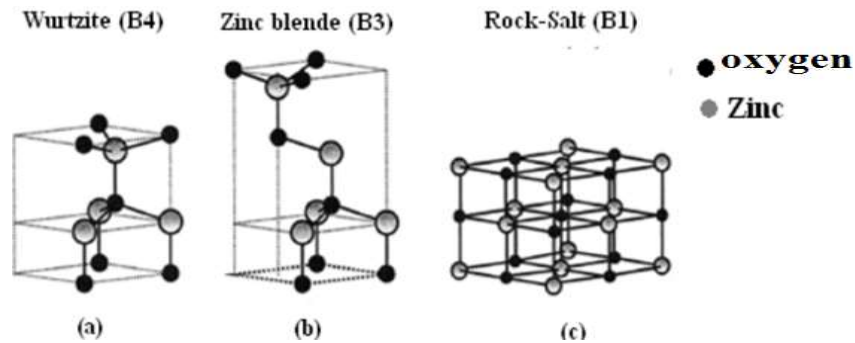
Figure I.15. Stick and ball representations of ZnO crystal structures [42]: **(a)** hexagonal würtzite (B4), **(b)** sphalerite structure (B3), and **(c)** Rock–Salt structure (B1).

The stable phase of ZnO is the hexagonal structure würtzite (B4). It consists of layers of zinc atoms alternating with layers of oxygen atoms along the c axis composed of O^{2-} and Zn^{2+} ions coordinated in tetrahedral form. All atoms have tetrahedral coordination with four nearest neighbors of the typical opposite [18]. It is anisotropic whose preferred axis of crystal growth is the c axis. Its structure can be described as two hc networks which are inserted into each other. Its space group is P63mc (Figure I.16).
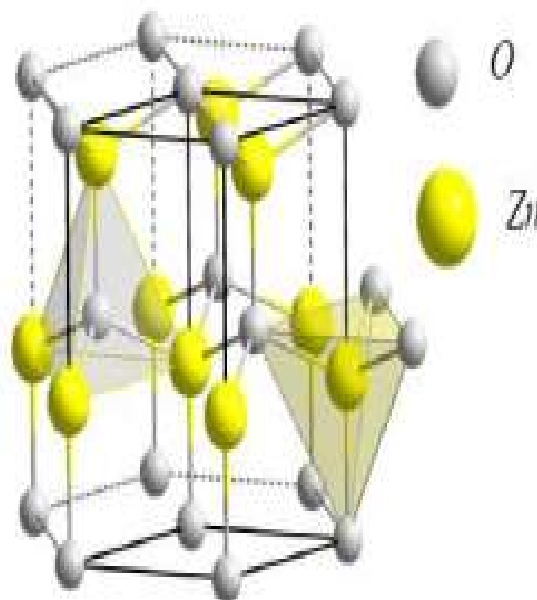
Figure I.16. Crystal structure of ZnO [45].

The O lattice is displaced by a fraction of 0.38 of the size of a unit cell in the direction. This displacement is performed relative to the Zn lattice. Indeed, the zinc and oxygen atoms occupy only 40% of the volume of the crystal, leaving empty spaces with a radius of 0.95 Å [4].

It is possible that, under certain conditions, excess zinc atoms can lodge in these spaces i.e. in interstitial position. This characteristic makes it possible to explain certain particular properties of the oxide, related to the phenomena of semi-conductivity, photoconductivity, luminescence, as well as the catalytic and chemical properties of the solid [30].

The distance between the near neighbors in the direction c, is smaller than for three other neighbors.

I.5.1.2. Optical properties of ZnO

Zinc oxide is a transparent material in the visible range in the massif case the refractive index is approximately 2 while in the case of thin films the refractive index ranges between 1.37 and 2.20 in terms of elaboration conditions, the fundamental absorption threshold being in the ultraviolet range (Figure I.17) [46].
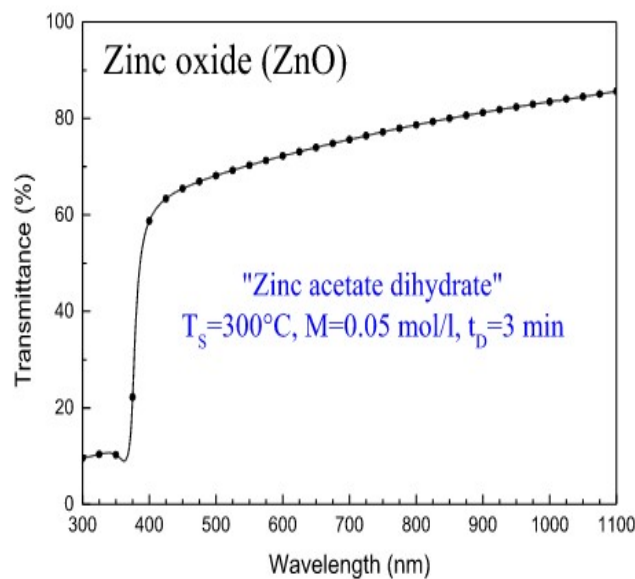
Figure I.17. The variation of transmittance with wavelength of zinc oxide deposited by spray pyrolysis [46].

The improvement of the stoichiometry of ZnO leads to a decrease in the absorption coefficient and an increase in the forbidden band energy [7,17], optical properties of ZnO are reported in the table I.3.

Table I.3. Some optical properties of ZnO [47,48].

Dielectric constant	8.7
Absorption coefficient (cm^{-1})	10^4
Refractive index at 560 nm	1.8-1.9
Refractive index in 590 nm	2.013-2.023
Excitonic band width (meV)	60
Transmittance in visible range (%)	~80

I.5.1.3. Electrical properties of ZnO

ZnO is a semiconductor of the group $A^{IV}B^{II}$, electron distribution of Zn and O atoms is:

$$O: 1s^2 2s^2 2p^4$$

$$Zn: 1s^2 2s^2 2p^6 3s^2 3p^6 4s^2 3d^{10}$$
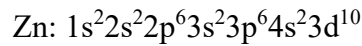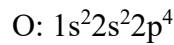
where the 2s and 2p states of oxygen, form the valence region and 4s states of zinc form the conduction region.

The ZnO owens a direct band gap. The minimum transfer band limit and the maximum valence band limit are at the point (the Brillouin area). ZnO has wide direct band-gap (3.3 eV) and it changes from 3.3 eV to 3.39 eV according to the type or the method of preparation or according to doping rate. On the other hand, ZnO has the widest excitonic band in the family II-VI (60 meV for ZnO, 20 meV for ZnS and 21 meV for GaN), which makes the excitonic effect observable even at room temperature.

The high concentration of electrons is attributed to the deviation from stoichiometry (or failing that in the structure), this deviation may be due to anion vacancies or to an excess of cations in the interstitial position. The exact nature of the structural defects in most cases is still uncertain. The stoichiometric ZnO formation reaction [7,25]:

$$Zn^{++} + 2e^- + \frac{1}{2}O_2 \rightarrow ZnO \tag{I.1}$$
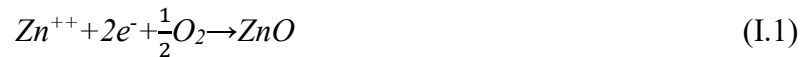
The zinc oxide films deposited with a spray pyrolysis have electrical conductivity ranging from $10^{-6} - 10^2 \ (\Omega.cm)^{-1}$ and it increase if the thickness increase, this causes an increase in the concentration of charge carriers. Heat treatment with gas or air affects the increase in conductivity. The spread of charge carriers is due to three factors [6,17,49]:

❖ The appearance of ionizing or neutral impurities,
❖ The appearance of grain boundaries in the material,
❖ The presence of optical or acoustic phonons.

Table I.4. Some electrical properties of ZnO [17,45,50].

Nature of the forbidden band	Direct
Band gap width at 4.2 K (eV)	3.3
Band gap width at 300K (eV)	3.34±0.02
Conductivity type	n
Maximum electron mobility (cm^2/V.s)	200
Effective mass of electrons	$0.28m_0$
Effective mass of holes	$0.60m_0$
State density in BC (cm^{-3})	3.71 10^{18}
State density in BV (cm^{-3})	1.16 10^{19}
Electron thermal velocity (cm. s^{-1})	2.2 10^7
Holes thermal velocity (cm. s^{-1})	1.5 10^7
Electrical resistivity (Ω.cm)	10^{-1}-10^6

I.5.2. Chromium oxide properties

There are many structures of chromium oxide such as [9,20]:

✓ Chromium (II) oxide,

✓ Chromium (IV) oxide,

✓ Chromium (III) oxide.

Chromium (II) oxide

Chromium (II) oxide (CrO) is an inorganic compound composed of chromium and oxygen. It is black powder that crystallizes in the rock salt structure (figure I.18) [51].
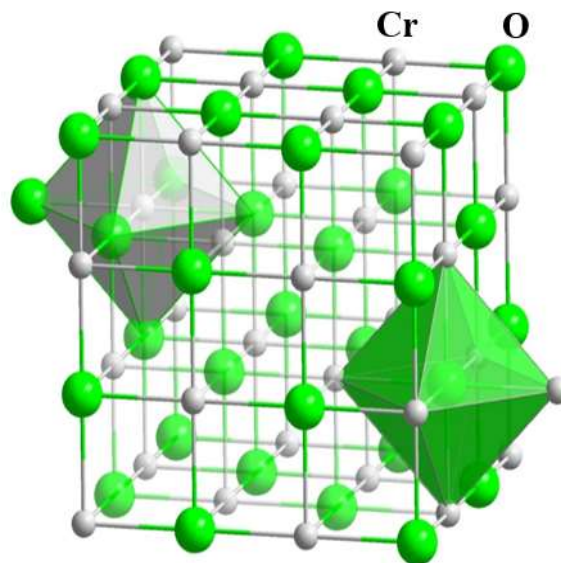
Figure I.18. CrO crystal structure.

Some physical properties are mentioned in the table I.5 [9].

Table I.5. Some physical properties of chromium (II) oxide (CrO) [9].

Properties	CrO
Molar mass (g/mol)	67.996
Appearance	Black
Melting point (°C)	300
Crystal structure	Cubic, cF8
Space group	$Fm\bar{3}m$

Chromium (IV) oxide

Chromium (IV) oxide (CrO_2) is an inorganic compound in the form of a crystal or powder of dark-brown color and insoluble in water (Figure I.19), it loses oxygen at 300 °C and it is a black synthetic magnetic solid. It once was widely used in magnetic tape emulsion. With the increasing popularity of CDs and DVDs, the use of chromium (IV) oxide has declined.

However, it is still used in data tape applications for enterprise –class storage systems. It is still considered by many oxide and tape manufactures to have been one of the best magnetic recording particulates ever invented [9].
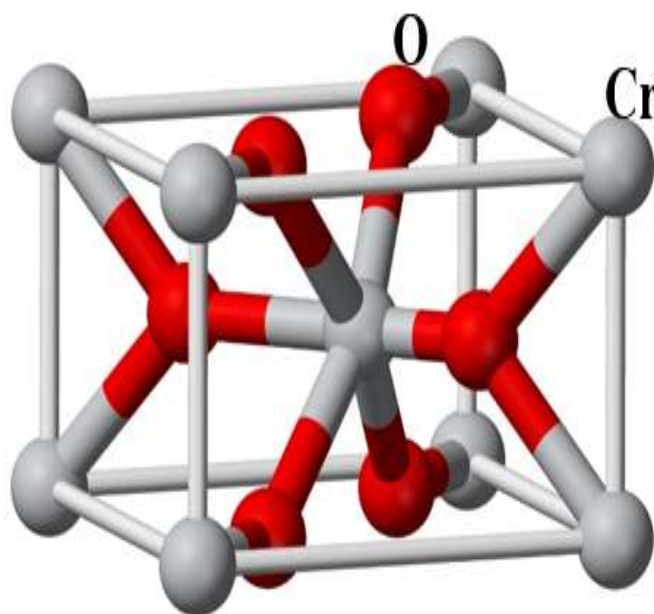
Figure I.19. CrO_2 Crystal structure.

We have grouped some physical properties of chromium (IV) oxide in the table I.6.

Table I.6. Some physical properties of chromium (IV) oxide (CrO_2) [11].

Properties	CrO_2
Molar mass (g/mol)	83.9949
Appearance	Black tetrahedral ferromagnetic crystals
Density (g/cm^3)	4.89
Melting point (°C)	375
Solubility in water	Insoluble
Crystal structure	Rutile (tetragonal), tp6
Space group	P4$_2$/mm
Residual resistivity (Ω.m)	10^{-8}
Absorption coefficient at 420 nm(cm^{-1})	$\sim 1.3 \times 10^5$
Inter band transition frequency (eV)	2.0 & 3.35
Real dielectric function, ε_1	2.9
Imaginary dielectric function, ε_2	3.8

Chromium (III) oxide

Chromium (III) oxide (Cr_2O_3) is an inorganic compound. This is one of the major oxides of chromium. Here, the metal has a +3 oxidation state.

The rare natural mineral of Cr_2O_3 is Eskolaite (**Figure I.20)**.

Figure I.20. The rare natural mineral of Cr_2O_3 (Eskolaite).

The Cr_2O_3 structure belongs to the R3c space group, which consists of hexagonal close-packed layers of O atoms, where two–thirds of the octahedral interstices between them are filled with Cr atoms. The oxygen atoms follow hcp packing (ababab…), while Cr atoms follow FCC packing (ABCABC…..) **(Figure I.21)** [11].
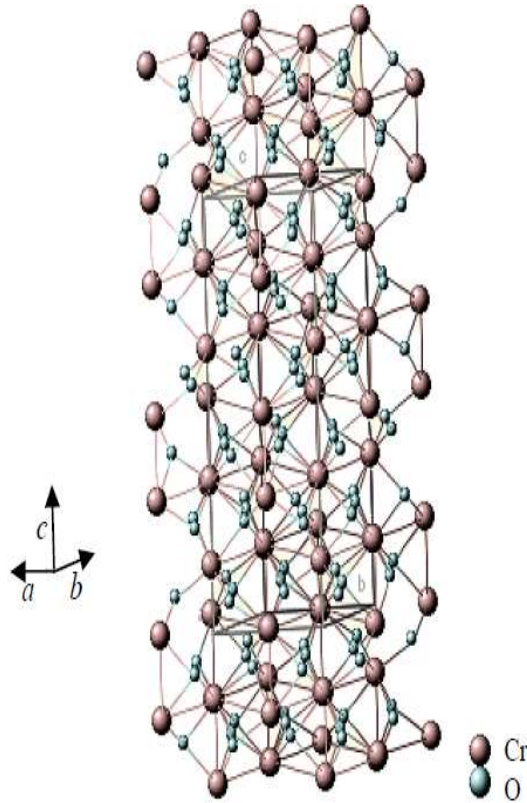
Figure I.21. Cr$_2$O$_3$ crystal structure [11].

The films are transparent in the wavelength range from 400 to 900 nm, but absorbing for wavelengths shorter than 400 nm (Figure I.22) [52].
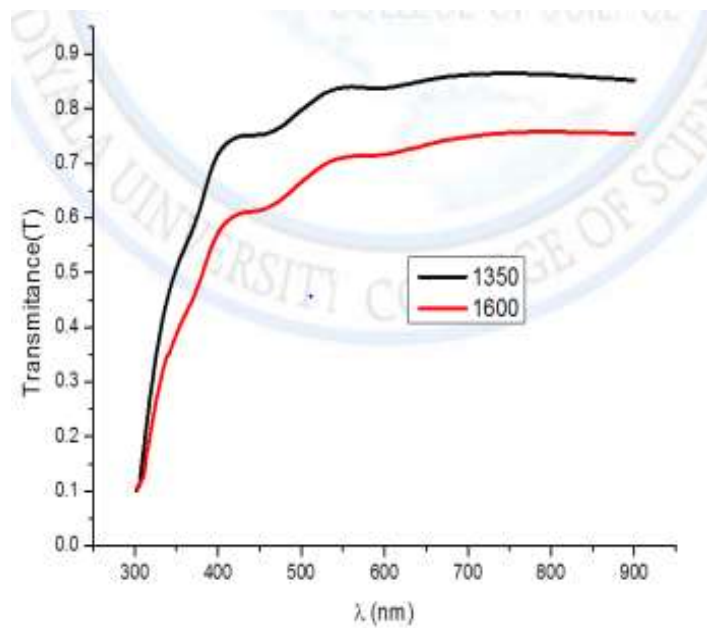
Figure I.22. Variation of transmission with wavelength of Cr$_2$O$_3$ at different films thickness [52].

The electron distribution of Cr and O atoms is:

$$O: 1s^2\,2s^2 2p^4$$

$$Cr: 1s^2 2s^2 2p^6 3s^2 3p^6 4s^1 3d^5$$
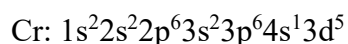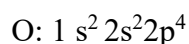
We have grouped some physical properties of chromium (III) oxide in the table I.7

Table I.7. Some physical properties of chromium oxide (Cr_2O_3) [9-11].

Properties	Cr_2O_3
Molar mass (g/mol)	151.99
Appearance	green powder or crystals
Density (g/cm^3)	5.22
Melting point (°C)	2435
Solubility in water	Insoluble
Space group	R3c
Lattice constant value (Å)	a =b=4.959, c=13.594
Transmittance (%)	50%
Refractive index	2.551
Absorption coefficient (cm^{-1})	0.97×10^4
optical band gap energy (eV)	3
The electrical conductivity at 500k (S.cm^{-1})	1×10^{-2}-2.5×10^{-3}
The activation energy (eV)	0.42-0.51
The large disorder energies (eV)	0.31-0.39

I.5.3. Zinc oxide applications

Because of its innumerable structural, optical and electrical properties, its production cost and the possibility of depositing it on large surfaces, ZnO is a very attractive material for various applications in the field of electronics and optoelectronics, the most important of which are [6,8,50]:

- Application to solar cells,
- Optoelectronic application in the visible and UV regions,
- Gas detectors,
- Piezoelectric applications,
- Surface acoustic wave device.

I.5.4. Chromium oxide applications

Chromium oxide is used as a pigment in the cosmetics industry, plastics, glass and also in paints and inks. It is also used in abrasive or polishing agents such as steel. Also, anhydrous chromic oxide is used for its heat, light and chemical resisting properties in applications such as [12]:

- Cement-based products such as industrial floors, concrete blocks, fired concrete bricks, tiles, slabs, joint mortar, terrazzo,…etc.
- Lime-based products such as mineral paint, frescoes, plasters, ornaments,…etc.

Chapter II

Elaboration and characterization of Cr-doped ZnO thin films

Chapter II: Elaboration and characterization of Cr-doped ZnO thin films

This chapter is divided into two parts, the first part will study the method of ultrasonic spray pyrolysis with the steps of preparing zinc oxide undoped and doped with chromium thin films. While the methods of optical and electrical characterization of our films will be studied in the second part.

Part One: Elaboration of Cr-doped zinc oxide thin films

II.1.1. Ultrasonic Spray Pyrolysis

Ultrasonic Spray Pyrolysis (USP) is a simple aerosol synthesis technique widely used for the synthesis of nano-materials such as thin films or Nanoparticles. Due to its easy feasibility, flexibility, and cost-effectiveness, the USP process is an important alternative for chemical solution deposition (CSD). The composition of the nano-synthetic particles or the film can be easily modified by changes in processing parameters. Ultrasonic spray pyrolysis gives you full control over the most important process parameters such as: ultrasonic amplitude, precursor solution, precursor composition, viscosity, flow rate, deposition temperature, and substrate temperature. This makes ultrasonic spray pyrolysis an attractive technology for dense and porous particles and thin film coating [2,4,5,15]

II.1.1.1. General principle of the ultrasonic spray pyrolysis process

The general principle of this technique depends on:

A solution containing the different constituents of the compound is sprayed in fine drops by a 40 KHz ultrasonic generator. It allows the transformation of the solution at the nozzle into a jet of very fine droplets 40μm in diameter. The jet arrives on the surface of the substrates which are heated which allows the activation of the chemical reaction. Under the appropriate experimental conditions, the vapor formed around the droplet prevents direct contact between the liquid phase and the surface of the substrate. This evaporation of the droplets allows a continuous renewal of the vapor, therefore the droplets undergo the thermal decomposition and give the formation of strongly adherent films. The experiment can be performed in air (~1 atm). And can be prepared in an enclosure (or in a reaction chamber) under vacuum (~0.1 atm). The description of film formation by the spray pyrolysis method can be summarized as follows [3,4,22] :

(1) Formation of droplets at the outlet of the nozzle,

(2) Transfer the droplets to the substrate surface,

(3) Decomposition of the precursor solution on the surface of the substrate heated by the pyrolysis reaction.

II.1.1.2 Choice of ultrasonic spray pyrolysis technique

Spray pyrolysis have several advantages [3,13] :

➢ It has being neither combustible nor explosive in the fire, or being relatively inert towards of the human organism,

➢ The speed and simplicity of implementation,

➢ It allows you to control the chemical composition of the material you want to obtain,

➢ Several products can be used at the same time, in particular for doping,

➢ The thin layers prepared by this technique are of good quality,

➢ It is a very inexpensive and economical technique. It can be industrialized,

➢ Deposits can be made by this method on large surfaces in case of solar cells or flat screens,

➢ It gives excellent adhesion of thin films to the substrate.

II.1.1.3. The effect of substrate temperature on droplets

According to figure II.1, several processes can occur depending on the range of used temperature [2,4]:

➢ **Schema A:** the droplet reaches the substrate, the solvent evaporates leaving a precipitate which then decomposes in the solid state.

➢ **Schema B:** the solvent evaporates before the droplet reaches the surface to be coated and the precipitate hits the substrate, decomposing into the solid phase.

➢ **Schema C:** As solvent evaporation occurs before contact with the hot substrate surface, the precursor passes into the gas phase without decomposition. The vapor thus produced during this process adsorbs and diffuses on the surface, then undergoes chemical reactions to form the layer. This process results in dense, good quality films with excellent adhesion.

➢ **Schema D:** at higher temperature, the chemical reaction no longer takes place in a heterogeneous phase, but in a homogeneous (gaseous) phase with the production of fine powder particles which can be deposited on the substrate. The deposit obtained has a high porosity and has a low adhesion to the substrate.

Therefore, the best layers are obtained with schema C which corresponds to the conditions of chemical vapor deposition. A wide droplet size distribution will lead to a mixed process.
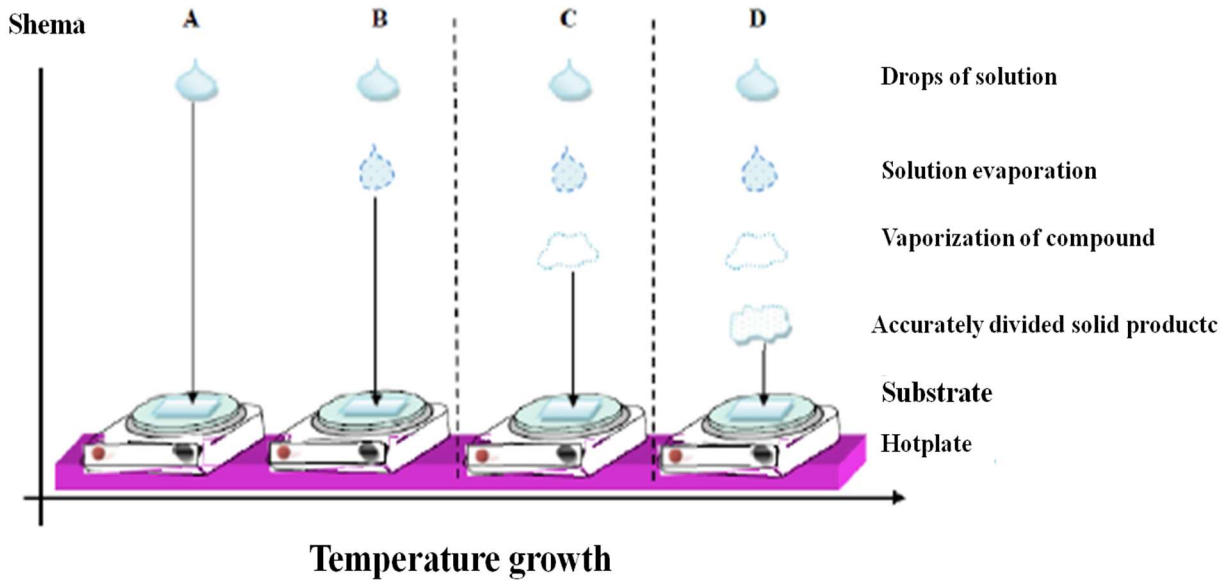
Figure II.1. Diagram of aerosol decomposition as a function of substrate temperature.

II.1.1.4. Generation and transport of droplets

The homogeneity of the deposited material can be determinate from the size of the spray droplets and the concentration of the solution while, its morphology can also be determined by the concentration and the speed of the droplets produced by the atomizers.

Concerning the atomizer, device for the production of droplets and their dispersions in the air. Several methods have been used to aid in the study of spray pyrolysis, for exemple: pneumatic (air is the carrier gas), ultrasonic, by gravity,…etc [5].

In the deposition device, the basic solution can be conveyed to the substrate under the effect of the compression of a gas sensitivity and the other hand, the gas used can also be used as reactive elements entering into the composition of the material to be deposited, such as O_2 for ZnO [5].

II.1.1.5. Reaction on substrate

When the aerosol droplets approach the surface of the heated substrate (at high temperatures) under the appropriate experimental conditions the vapor formed around the droplet prevents direct contact between the liquid phase and the substrate of the droplets allows a continuous renewal of the vapor, therefore the droplets undergo the thermal decomposition and give the formation of strongly adherent films.

It is noted that the decomposition reaction, in the gas phase, occurring on the surface of the substrate is an endothermic reaction which requires relatively high substrate temperatures to cause the decomposition of the droplets, and give rise to the growth of the film [5].

II.1.2. Experimental procedure

The objective of this work is to develop thin films of undoped zinc oxide (ZnO) and chromium doped zinc oxide (ZnO:Cr) by the technique of ultrasonic spray pyrolysis.

Where, the experimental variables (substrate temperature (T_S), deposition time (t_D), solution concentration (C) and solution flow rate (φ_S) were kept constant throughout the sedimentation process with two different distances between the nozzle and the substrate (d_{N-S}) for studied the effect the chromium concentration and Nozzle-substrate distance on the properties of ZnO thin films deposited by spray pyrolysis.

-In this study, the two solutions (A and B) were prepared from:

A. Zinc acetate dihydrate $Zn(C_2H_3O_2)_2 \cdot 2H_2O$.

B. Chromium chloride hexahydrate ($CrCl_3 \cdot 6H_2O$).

By dissolving them in distilled water

Then, the two solutions were mixed in different volumetric (or atomic) proportions for the deposition of ZnO thin films with different doping by Cr.

II.1.2.1. Experimental setup

This experiment was carried out at the level of Laboratory of Materials and Structure of Electromechanical Systems and their Reliability (LMSSEF: *Laboratoire de Matériaux et Structure des Systèmes Électromécanique et leur Fiabilité*) of the Larbi Ben M'hidi University of Oum El Bouaghi, where, undoped and chromium-doped zinc oxide thin films were deposited by ultrasonic spray pyrolysis technique. The schematic diagram of the deposition system is shown in Figure II.2 and II.3.

Figure II.2. Complete experimental device for the ultrasonic spray pyrolysis technique.
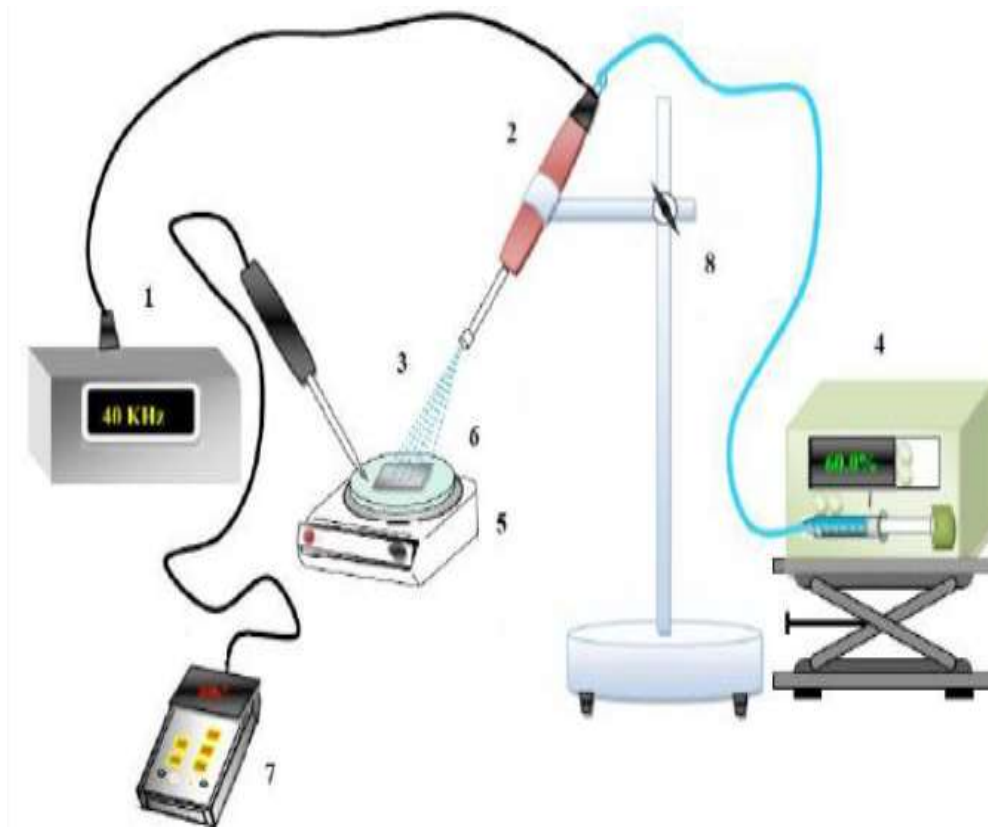
Figure II.3. Simplified diagram of the deposition of thin films by ultrasonic spray pyrolysis technique.

Table II 1. Presentation of the devices that the simplified diagram of USP system consist.

(1)	(2)	(3)	(4)	(5)	(6)	(7)	(8)
Ultrasonic Generator (40kh)	Ultrasonic atomizer	The spray	Syringe pump	Substrate heater	Substrate	Digital thermometer	Support

The main elements of the assembly are:

a) **Substrate heater**: It is a plate with a diameter of 25cm, heated by the Joule effect, the temperature used in our experiment is 400°C,

b) **Electric syringe pump**: Model PHOENIX D-CP (GF-FOURES) to control the precursor solution flow rate,

c) **Substrate**: in this work, microscopic glass substrates were used,

d) **Ultrasonic wave generator (40 KHz) with an atomizer:** Which allows to transform the solution at the level of the atomizer to very small droplets thin, placed on a height-adjustable support to control the spout-substrate distance,

e) Digital thermometer: It is a device for measuring the temperature, it allows you to give a direct reading of the temperature using a digital display, where, in this work the thermocouple tip (type K/NiCr-NiAl) is connected to the heater.

II.1.2.2. Choice and preparation of substrates

The type of substrate is chosen as glass according to:

1. Coefficient of thermal expansion: $\alpha_{Glass}=8.5\times10^{-6}$ K^{-1}and $\alpha_{ZnO}=7.2\times10^{-6}$K^{-1},

2. Not expensive,

3. Transparent for the optical characterization of films in the visible,

4. Better adhesion, good structure and better piezoelectric activity.

In order to deposit the thin films, glass microscope slides were used with dimensions (7.62×2.54) cm^2 and a thickness of 1mm. Where, each slide was cut into three using a diamond tip pen to obtain three substrates (Figure II 4).

Figure II.4. Slides of glasses are cut by a diamond tip pen to obtain substrates.

After obtaining the substrates, they must be cleaned as a basic step follows **(Figure II.5)**:

- Rinsing with distilled water,
- Soaking in an acetone bath,
- Rinsing in distilled water bath to avoid remaining traces of acetone,
- Soaking in an ethanol bath,
- Cleaning with distilled water to remove traces of ethanol,
- Finally, these substrates are drying using Joseph papers **(Figure II.5.b).**

The degreasing in each bath lasts five minutes at room temperature in an ultrasound cleaning bath (**Figure II.5.c**).
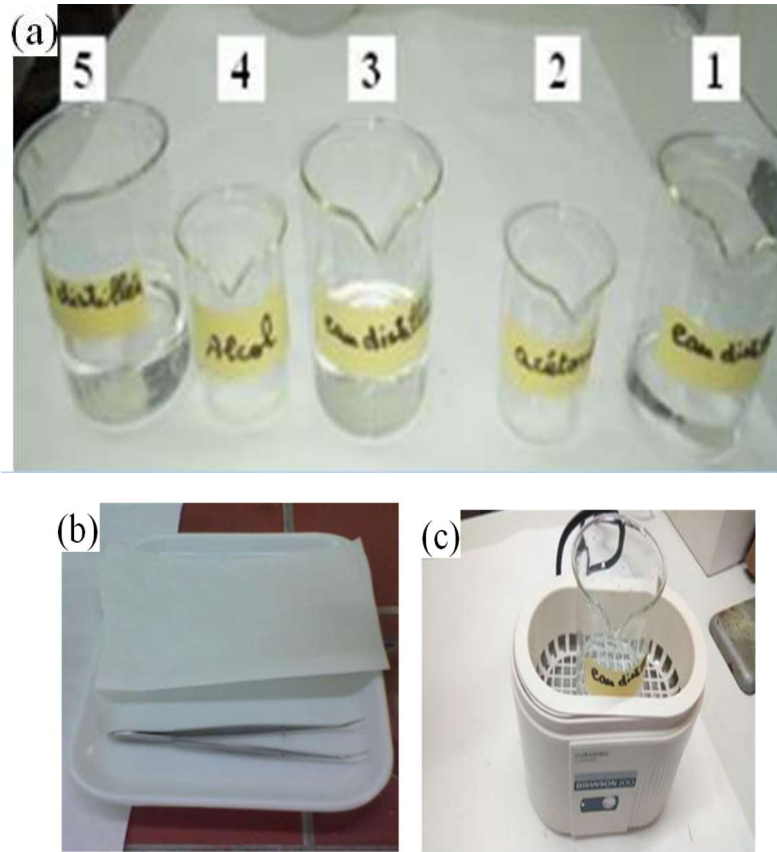
Figure II.5. Substrate's cleaning steps with some used tools.

II.1.2.3. Preparation of deposition solutions

a. Preparation of zinc acetate solution

There are several sources of zinc oxide such as: zinc acetate $Zn[OOCCH_3]_2$, zinc nitrate $Zn(NO_3)_2$ and zinc chloride $ZnCl_2$ [7]. In this work, zinc acetate dehydrate (ZAD) was used as a source of zinc material (Figure II.6).

Figure II.6. Zinc acetate dihydrate.

Table II.2. Some physical properties of ZAD [22,25].

Appearance	Crystalline solid
Color	White
Odor	Acetic acid odor
Molecular formula	$Zn(C_2H_3O_2)_2 \cdot 2H_2O$
Molar mass (g/mol)	219.50
Density (g/ml.) at 20°C.	1.735
Melting point (°C)	237

To obtain a solution from zinc acetate dihydrate (V_{ZAD}) of molar mass 219.50g/mol and concentration C=0.05mol/l, a quantity of zinc acetate ($m_{ZAD}=C_{ZAD}M_{ZAD}V$) was dissolved in distilled water (Figure II.7), where, a scale was used KERN442-432N accurately± 0.01g to weigh a certain amount of ZAD (m_{ZAD}).
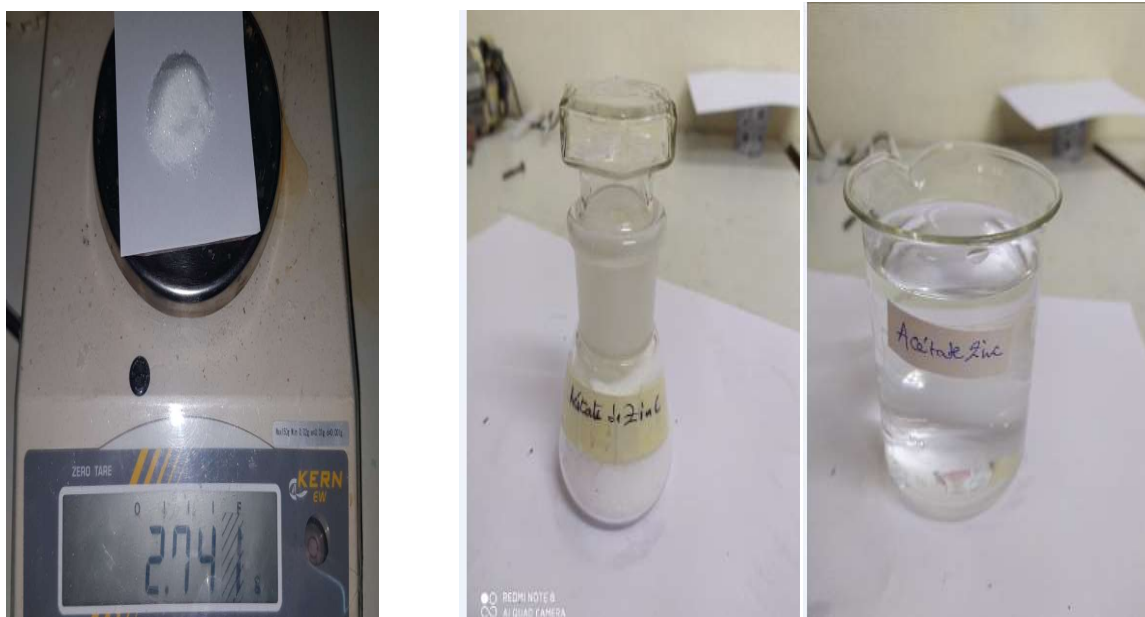
Figure II.7. Preparation of zinc acetate solution.

We note that zinc acetate dissolves well and completely in water, as we get a homogeneous solution with a transparent color.

b. Preparation of chromium chloride solution

In this work we used a chromium chloride hexahydrate ($CrCl_3 \cdot 6H_2O$) as a source of Cr material (Figure II.8).

Figure II.8. Chromium chloride hexahydrate.

Table II.3. Some physical properties of CrCH [9,10,20,51].

Appearance	Crystalline solid
Color	Dark green
Solubility in water at 20°C (g/100ml)	59
The molecular formula	$CrCl_3 \cdot 6H_2O$
Molar mass (g/mol).	266.5
Density at 20°C (g/cm^3)	2.76
Melting point (°C)	83-95

To obtain a solution from chromium chloride hexahydrate (V_{CrCH}) of molar mass 266.5g/mol and concentration C=0.05mol/l, a quantity of chromium chloride hexahydrate ($m_{CrCH}=C_{CrCH}M_{CrCH}V$) was dissolved, in distilled water (Figure II.9), where the previous balance was used to weigh a certain amount of C_rCH (m_{CrCH}).

We note that chromium chloride hexahydrate dissolves well and completely in water, as we get a homogeneous solution with a green color.

Figure II.9. Preparation of chromium chloride solution.

c. Preparation of precursor solution

After preparing the two solutions, a quantity of $(1-Z)V_{Sol\ ZAD}$ from zinc acetate dihydrate solution is mixed with a quantity of $ZV_{Sol\ CrCH}$ from chromium chloride hexahydrate solution to prepare a $Zn_{1-Z}Cr_ZO$ as precursor solution for preparing samples of zinc oxide thin films doped at Z% by chromium atoms.

II.1.2.4. Experimental condition

To study the doping effect and nozzle-substrate distance, a variety of samples has been produced under experimental conditions presented in the table II.4.

Table II.4. The experimental conditions of the deposition series.

Conditions	Values
Nature of precursor	$Zn(C_2H_3O_2)_2 \cdot 2H_2O$ $CrCl_3 \cdot 6H_2O$
Solvent	H_2O
Molarity of the solution (mol/l)	0.05
Volume of soution for each deposit (ml)	10
Substrate temperature (°C)	400
Solution folow (ml/h)	60
Nozzel-substrate distance (cm)	4,6
Deposition time (min)	6
Doping rate (*at.* %)	0, 2, 4, 6, 8

II.1.2.5. Deposition of thin film

After the preparation of the substrates and the deposition solutions, the procedure for depositing the samples comes all according to the following steps [3,4,15]:

-First, the precursor solution is placed in the syringe, and the latter is placed in the syringe pump device on the other hand the glass substrates are placed above an electrical resistance at room temperature to avoid thermal shock.

-Second, the substrates are gradually heated to the chosen deposition temperature (400°C), the temperature value is measured by a digital thermometer.

-Third, when the heating is done, the flow rate of the solution (φs) is fixed using an electric syringe pump. In our work, we used the amplitude of the sound wave (60%) and the type of continuous pulse.

Very fine droplets of the precursor solution are sprayed, by ultrasonic, on the heated substrate which causes the activation of the chemical reaction between the compounds, the solvent evaporates due to the endothermic reaction of the three compounds forming the thin film.

-Finally, after 6 min, the spraying of solution and the heating are stopped but we let the deposition samples cool down above a resistance electric up to room temperature, to avoid thermal shocks that could break the sample.

Thus, transparent samples well adhered to the substrate were obtained.

Part two: Characterization techniques of thin films

II.2.1. Optical characterization and measurement

There are several ways to characterize transparent conductive films, including methods (structural, electrical and optical) that help in obtaining several properties including (band gap, absorption coefficient, grain size, thickness and Urbach energy) for thin films [1]. Which is obtained by studying the transmission spectrum (optical transmittance curve as a function of wavelength) data given by UV-Vis Spectrophotometer.

II.2.1.1. Ultraviolet-visible spectroscopy

Ultraviolet-visible spectroscopy is a non-destructive optical characterization technique based on the transition of electron from fundamental state to an excited state due to excitation by an electromagnetic wave [1,53].

This technique allows working on small amounts of materials deposited in thin films or in suspension it refers to absorption spectroscopy or reflectance spectroscopy in the ultraviolet-visible-near infrared spectral region. The absorption or reflectance in the visible range directly affects the perceived color of the chemicals involved; it measures the intensity of light passing through a sample (I) and compares it to the intensity of light before it passes through the sample (I_0). The ratio (I/I_0) is called the optical transmittance and it is usually expressed as a percentage (T %). This technique can provides information on the optical properties besides what it mentioned previously such as optical absorption coefficient (α), the estimation of optical gap (E_g), Urbach energy (E_{Urb}) and optical refractive index (n, k). It can also in certain cases give information about the thickness of studied sample [2,13,53].

To obtain the optical properties of our samples a double beam recording spectrophotometer type (V-630) are used one passes through the reference (air) and the other through the sample (glass+layer) so the output intensities amplified spectra are processed using UVPC software

(Figure II.10). Then, we managed to record curves representing the variation of the transmittance as a function of the wavelength in the Ultra-Violet and Visible range. The exploitation of these curves makes it possible to determine optical characteristics such as the optical absorption threshold, the absorption coefficient.

Figure II.10. Experimental device for UV-Vis-NIR spectroscopy.

Figure II.11 shows the principle of UV-Vis- NIR spectrophotometry.
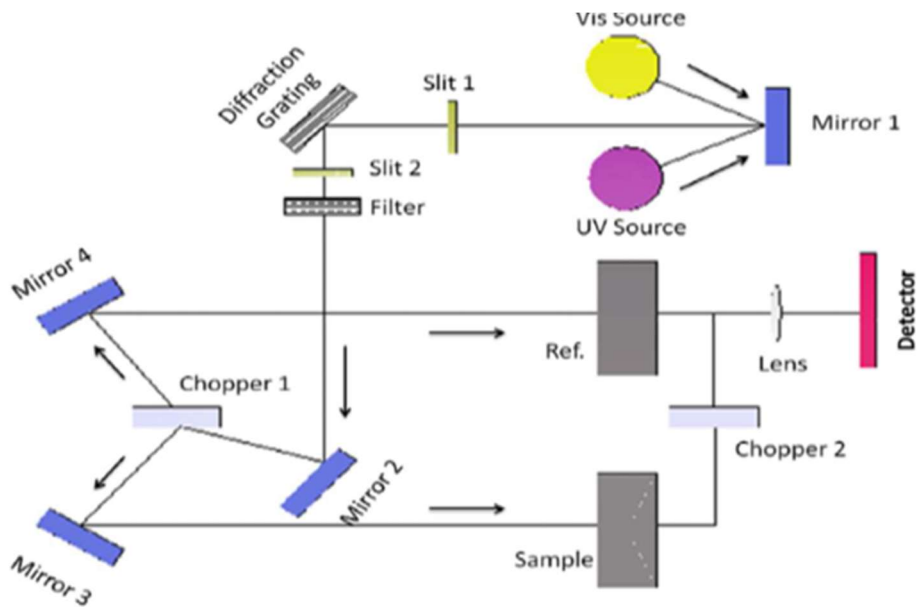
Figure II.11. Schematic spectrometer of UV-Vis-NIR [1].

We were able to obtain spectra representing the variation of optical transmittance T (%) according to the wavelength in the UV-Visible-NIR range (300 nm- 1100 nm).

II.2.1.1.1. Determination of film thickness and refractive index

The thickness of a thin layer is very low, and its knowledge necessary, it seems legitimate to specify it first [3].

We determine the thickness of our films of ZnO:Cr (0, 2, 4, 6 and 8 *at.* %) from the spectrum of the variation of the optical transmittance of each sample (film + glass) as a function of the wavelength by adjusting a transmittance curve calculated according to a model proposed by Swanepoel to the measured transmittance spectrum and this by varying certain parameters, such as the thicknesses, and to use the least squares method for fit a simulated transmittance curve to the measured one [3,4]. From the "Fit" of the transmittance curve using the Origin Pro 8.5 software, one can determine the average thickness of the thin film, the refractive index as well as the extinction coefficient and the corresponding wavelength to the optical gap (Figure II.12).
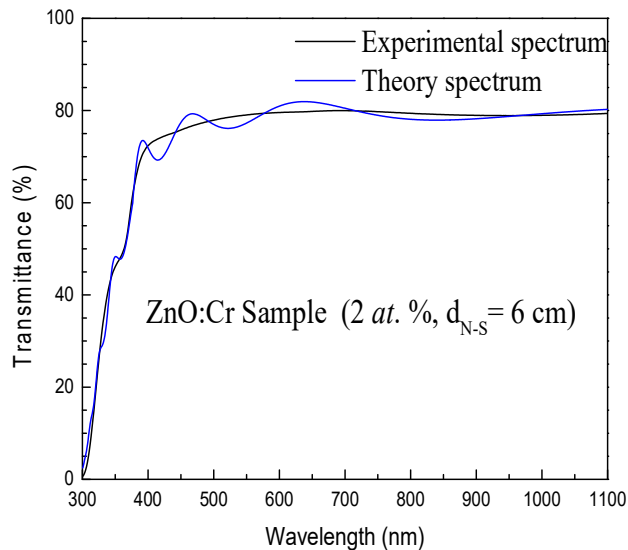
Figure II.12. Fitting the measured transmittance spectra to Swanepoel's method.

II.2.1.1.2. Determination of absorption coefficient

When the UV-Visible spectrum passes over the sample, some rays do not pass through the thin film, but they are absorbed by this film (negligible reflection).

In the spectrum domain where light is absorbed and knowing the film thickness (t), the absorption coefficient of the film can be determined as a function of the wavelength according to Beer-Lambert law [13]:

$$T = e^{-\alpha.t} \tag{II.1}$$

$$\alpha = \frac{1}{d} ln\left(\frac{100}{T(\%)}\right) \tag{II.2}$$

II.2.1.1.3. Determination of optical band gap

The term "band gap" refers to the energy difference between the top of the valence band to the bottom of the conduction band electrons are able to jump from one band to another.

In order for an electron to jump from a valence band to a conduction band, it requires a specific minimum amount of energy for the transition, the band gap energy [1].

The optical energy band gap (E_g) for the allowed transition between the conduction and valence bands can be found from the Tauc equation [14]:

$$(\alpha h\upsilon)^n = A(h\upsilon - E_g) \tag{II.3}$$

where:

$h\upsilon$: Energy of incident photon (eV).

A: Constant dependent on electron-hole mobility.

E_g: Energy of the optical gap (eV).

In the case of a thin film of undoped and doped zinc oxide (ZnO), the direct optical gap n=2 [6], from Tauc's law, we plot the curve $(\alpha h\upsilon)^2$ as a function of hυ (Figure II.13). The value of the optical gap is determined by extrapolation of the curve up to $(\alpha h\upsilon)^2 = 0$. The point of intersection with the horizontal axis indicates the value of the optical gap.
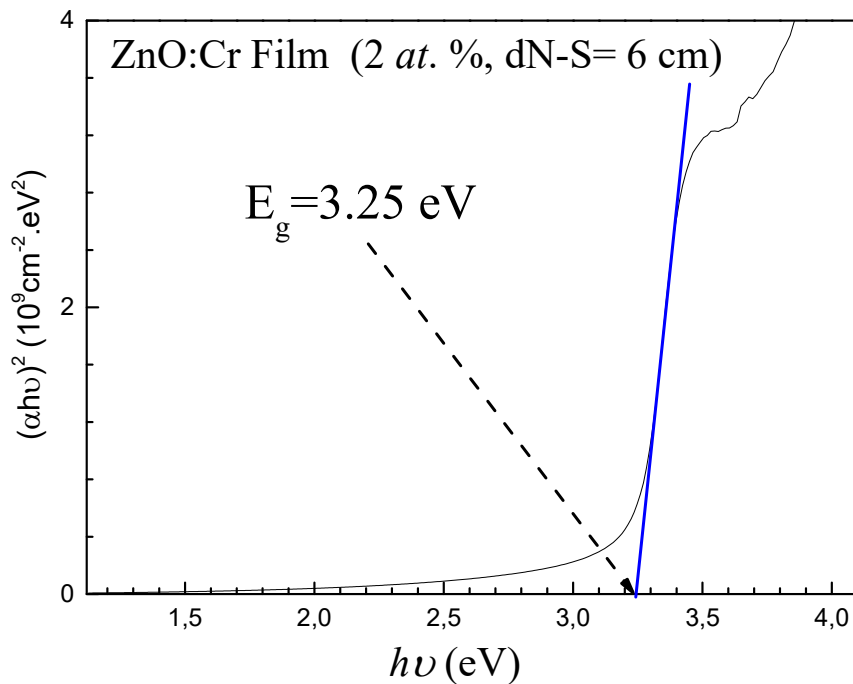
Figure II.13. Example of the determination of the energy gap from the variation of $(\alpha h\upsilon)^2$ as a function of hυ.

II.2.1.1.4. Determination of Urbach energy

Due to disorder in the film lattice, localized states appear near band edges which cause band tailing. These bands are responsible for the absorption of photons in the low energy range. In this range, the absorption coefficient is given by Urbach's law [15,54,55]:

$$\alpha = \alpha_0 exp\left(\frac{h\upsilon}{E_{Urb}}\right) \tag{II.4}$$

where, α: The absorption coefficient, α_0: is the pre-exponential factor, $h\upsilon$ the energy of the incident photon and E_{Urb} the tail band width or the disorder energy commonly called the Urbach tail [15,38,54].

By plotting $ln\alpha$ as a function of $h\upsilon$ (Figure II.14), E_{Urb} can be estimated from the inverse slope of the linear curve of lnα against hυ as shown in Equation II.5.

$$ln\,\alpha = ln\alpha_0 + \frac{h\upsilon}{E_{Urb}} \tag{II.5}$$
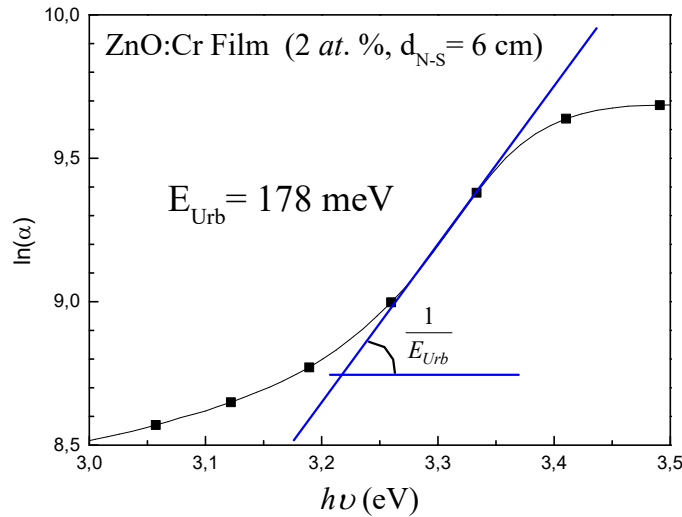
Figure II.14. Example of the determination of the Urbach energy.

II.2.2. Electrical characterization and measurement

Electrical properties cover a particularly wide field, the electrical properties of thin films are one of their most important physical features, especially the conductivity/resistivity [2]. To reliably determine the resistance of the manufactured layers, a four-terminal sensing method was applied [1].

The four-point probes method is a simple and fast method, which measures the electrical conductivity of thin films Figure II.15. Its principal is using four tips (probes), equidistant in direct contact with the surface of the sample, placed linearly in a straight line at equal distance (d) from each other.

The principle of measurement is simple, just inject a current (I) at the two external tips and measure the voltage (V) at the two internal tips [2].

Since each pair of the four pins was equidistant during the measurement, and the thickness of the layer is much smaller than its lateral dimension as well as the distance between the pins, the sheet resistance (ρ) can be calculated by the taking reciprocal of the slope of the I-V curve which calculated as follows in the equation [13]:

$$\rho = \beta \, \frac{V}{I} \qquad (II.6)$$

where, β is a geometry factor and in the case of semi-infinite thin film, β=4.53, which is just π /ln 2

Therefore, the electrical conductivity is related to the thickness of the films by the expression [56]:

$$\sigma = \frac{1}{\rho.t} \qquad (II.7)$$
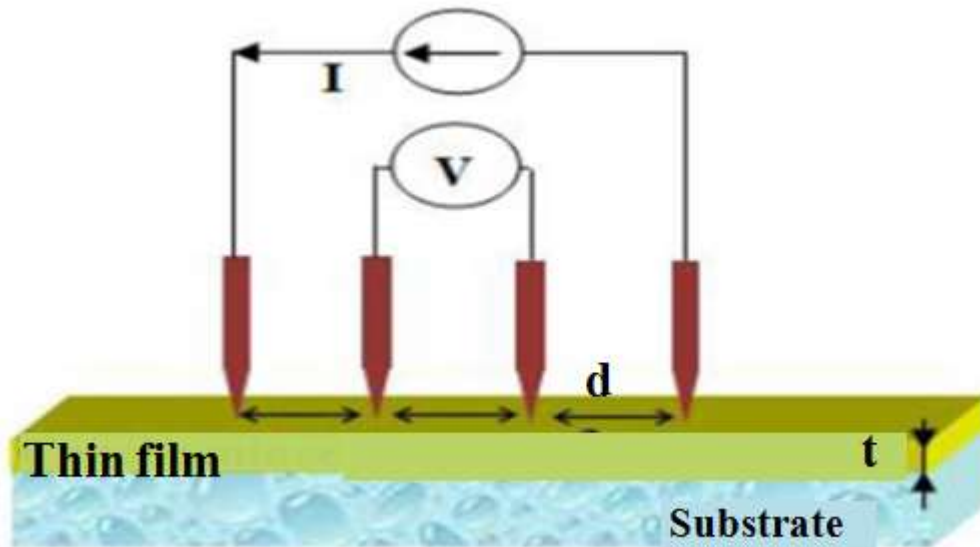
Figure II.15. Diagram representative of the principle of the four-point probes method [3].

In order to know the electrical surface resistivity ρ and electrical conductivity σ of undoped and doped zinc oxide (ZnO) of thin films, a four-points device type **Mandel** is used in the LMSSEF laboratory of Larbi ben M'hidi University at Oum Bouaghi, the probe consists of four contacts aligned linearly and the distance between the four terminals (d=1mm). A variable current I is applied between the two external terminals and the voltage V is measured between the two internal probes using **keitheley 2400**, which makes it possible to measure low voltages (**Figure II .16**).

Figure II.16. Four-point probe + Source Meter.

Chapter III

Results and discussion

Chapter III: Results and discussion

The purpose of this chapter is to present and interpret the experimental results of our work on the development and characterization of thin films of zinc oxide undoped and doped with chromium (ZnO:Cr) deposited on glass substrates by the ultrasonic spray pyrolysis technique We present the percentage effect of chromium doping and the effect of distance (d=4 cm and d=6 cm) on the optical and electric properties of the thin films of zinc oxide (ZnO) doped with different percentages of chromium (Cr) (0, 2, 4, 6, and 8 *at.* %) with constant deposit conditions (T_S, t_D, and φ_S).

To study these properties, we used two techniques to characterize our samples which are:

➢ UV-Visible-NIR spectrophotometry to discuss the spectrum of the transmittance and calculate from this spectrum: the thickness of the film(t), the absorption coefficient (α), the optical gap energy (E_g), the Urbach energy (E_{Urb}), and the refractive index (n) of our samples.

➢ The four-point technique to determine the type of majority charge carriers and measure the electrical conductivity of our samples.

III.1. Effect of Cr-doping of and nozzle-substrate distance on the color of ZnO samples

The table III.1 shows the photos of our samples, we notice that there is a very slight change in the color of the samples and they appear almost as if they are transparent in visible range because undoped and (Ni, Sn, Cr)-doped ZnO have a higher transparency in this range [5,7,57].

Table III.1. Photos of thin films deposited on glass substrates.

Cr·Concentration (at.·%) d_{N-S}	Glass Substrate	0	2	4	6	8
4cm.						
6cm.						

III.2. Effect of Cr-doping and nozzle-substrate distance on the optical transmittance of ZnO samples

We use the UV-Vis-NIR spectrophotometer (V-630) to study the optical properties of our samples; we were able to obtain spectra representing the variation of optical transmittance according to the wavelength in the UV-Visible-NIR range (figure III.1).

Figure III.1. Optical transmittance spectra of ZnO samples at different percentage of Cr prepared at two different nozzle-substrate distances (a): 4 cm and (b): 6 cm.

Figure III.1 represents typical spectra of the variation in optical transmittance T (%) as a function of the wavelength of the incident photon λ in the UV-Vis-NIR range, recorded in the range from 300 to 1100 nm obtained of zinc oxide sample prepared by the ultrasonic spray pyrolysis technique, with different percentage of Cr at 4 cm (Figure III.1.a), and 6 cm (Figure III.1.b) with the precise experimental conditions (T_S=400°C, T_D=6 min).

Two fields of optical transmittance can be distinguished according to the wavelength:

A region of strong absorption and low optical transmittance, which corresponds to the fundamental absorption due to the inter-band electronic transition (Figure I.2),which is presented in the higher photon energy region (ultraviolet region).
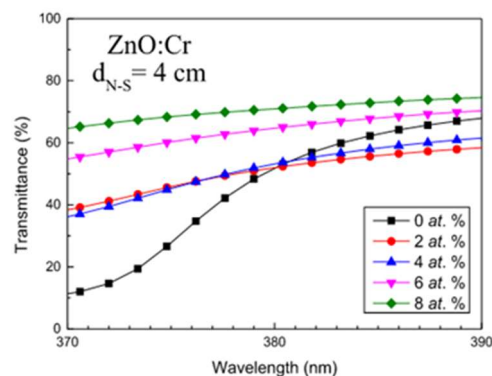
Figure III.2. Optical transmittance spectra in UV range of ZnO samples at different percentage of Cr.

We can interept this observation that at shorter wavelengths (λ< 400 nm), the absorbing region is attributed to the large exciton binding energy and the incident photon has more energy to interact with material atoms and thus, more photons are absorbed [57].

A region of strong transparency is located between 400 and 1100 nm (visible and near-infrared region). We observe that the stability of the transparency of our samples in the this field in the two both distance where the value of the transmission is about 60-80 % in 4cm and about 60-85% in 6cm. This results are very similar to some previous works (Figure III.3) which interepted that for longer wavelengths (λ> 400 nm) no light is scarttered or absorbed as a non-absorbing region [57,58].
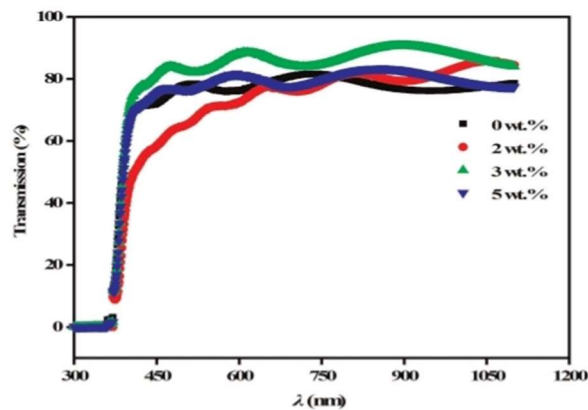
Figure III.3. Optical transmittance spectra for undoped and Cr-doped ZnO [57].

Figure III.4 (a &b) represents typical spectra of the variation in optical transmittance as a function of the wavelength of the incident photon in the UV-Vis-NIR range, recorded in the range from 300 to 1100 nm obtained of zinc oxide thin films prepared onto glass substrate by ultrasonic spray pyrolysis technique.
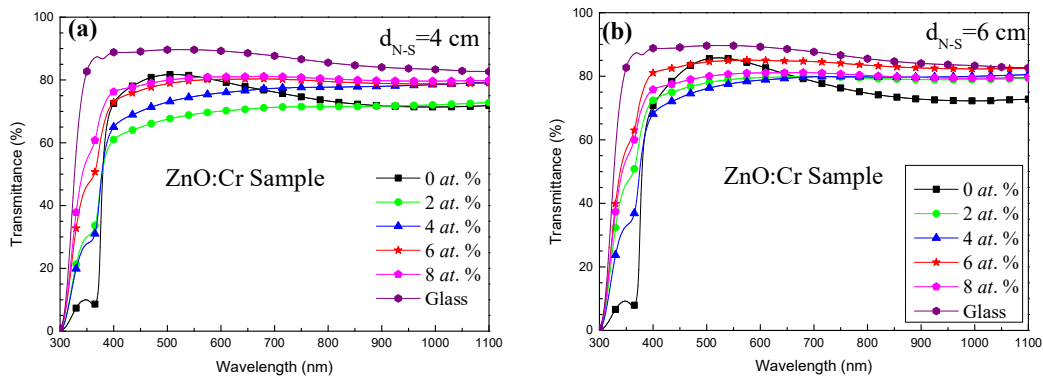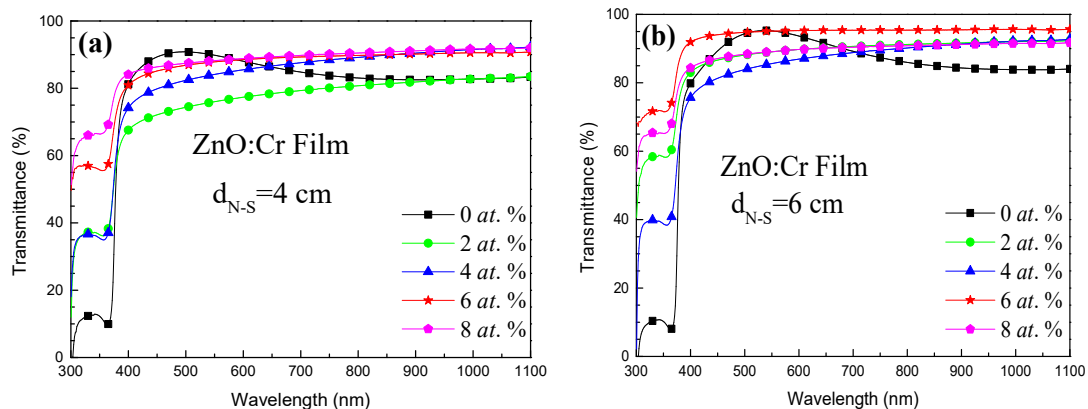

Figure III.4. Optical transmittance spectra of ZnO thin films at different percentage of Cr prepared at two different nozzle-substrate distances (a): 4 cm and (b):6 cm

The optical transmittance of undoped and doped zinc oxide (ZnO:Cr) thin films slightly increasing by the increasing of different percentages of chromium and also by increasing the nozzle-substrate distance.

- At 4 cm: we observed a slightly increase in transparency noting that at 2 *at*. % it is less transparent and the regression approaches the range UV with increasing of Cr doping percentage.

- At 6 cm, we noticed that most transparent is at 6 at. %.

We can interpret the slightly increasing in the transmittance in the visible range by [59]:

- The material does not absorb light in this field due to the transparency of ZnO, Cr_2O_3 and Cr_xO_y (Figure I.16 and I.21),

- The presence of voids and gaps on the surface of the substrate,

- May be due to scattering effects caused by the microrod microstructure of the deposit which presents a very non-planar surface (Figure II.12), films having smoother surface morphology generally show higher transmittance.

III.3. Effect of Cr-doping and nozzle-substrate distance on the film thickness of ZnO samples

We estimated the average thickness of our films from the variation of the optical transmittance according to the wavelength of the incident photon in the UV-Vis-NIR domain using the Swanepoel method which gives highly convergent values.

Figure III.5 shows the variation of the thickness of our thin films as a function of the doping concentration prepared at two different distances between nozzle and substrate. It is noted that the thickness values are between 410 and 490 nm at 4 cm and between 355 and 485 nm at 6 cm.
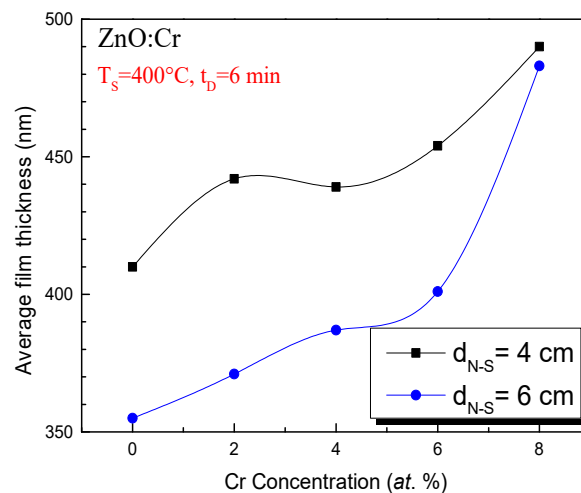
Figure III.5. Variation of average film thickness with Cr concentration.

According to the doping percentage for the same d_{N-S}, we can see a proportion between increasing of average thickness of zinc oxide thin films and increasing in chromium concentration (*at. %*). Because the thickness always increase by the increasing of doping even though the type of preparation method and the type of the doper (NiO:Cu, CuO:Ni, ZnO:Ni…) [3,5,6,60]. The increase of film thickness may be due to the increase in the porosities in the deposited material (ZnO:Cr) which makes the material become less density compared to undoped ZnO.

According to the nozzle-substrate distance for the same doping percentage, we noticed that there is an inverse relationship between the distance and the thickness.

We can interpret the large thickness of prepared films at d_{N-S} =4 cm by the presence of a much main amounts of material deposited i.e there is more material that contributes to the formation of the films (Zn,Cr), in contrast for another distance (d_{N-S}=6cm) where failure of the required amount of the precursor solution to reach the far substrate [13].

III.4. Effect of Cr-doping and nozzle-substrate distance on the refractive index of ZnO samples

Figure III.6 shows the variation of refractive index of ZnO:Cr thin films with the percentage of doping at two different nozzle-subsrtate distances.
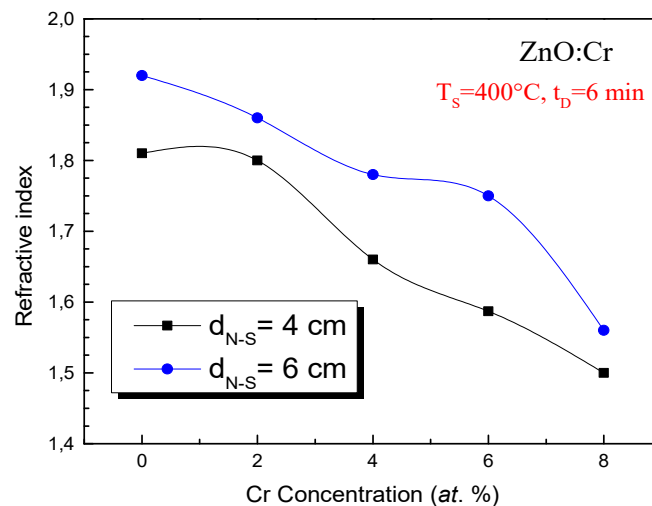
Figure III.6. Variation of refractive index of ZnO:Cr thin films with the percentage of doping at two different nozzle-substrate distances.

According to the doping percentage, we observe that the refractive index decrease with the increasing of doping percentage from 1.8 to 1.5 and from 1.925 to 1.55 at 4 cm and 6 cm, respectively.

This decreases by the increasing of doping percentage or decreases of d_{N-S} it may be due to the presence a large number of porosities hence to the small density of material.

Looking at the data presented in Figure III.7, we can see how thickness and refractive index of ZnO thin film varies with Cr concentration doping. It is clear that the refractive index decreases monotonically with increasing thickness of the film. This behavior can be due to the existence of more porosity in the film [61].
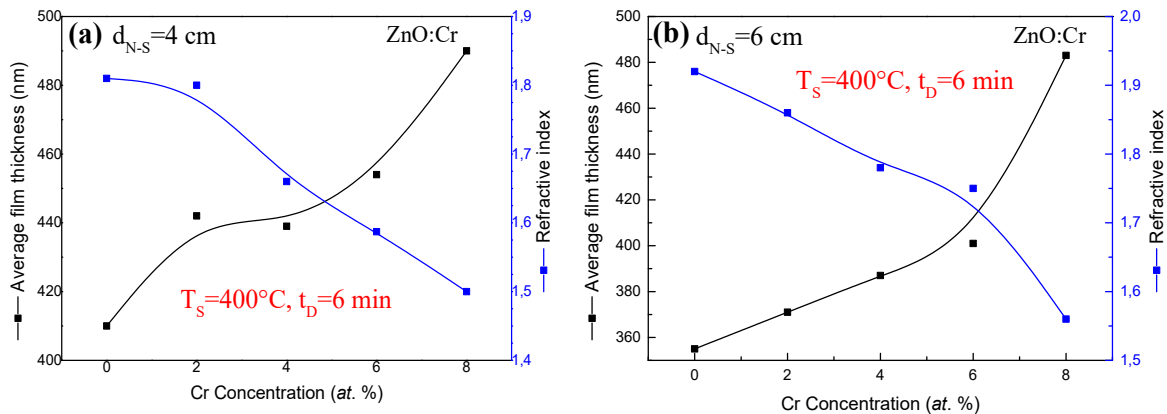
Figure III.7. Variation of thickness and refractive index of ZnO thin films versus Cr concentration at: **(a)** d_{N-S}=4 cm and **(b)** d_{N-S}=6 cm.

III.5. Effect of Cr-doping and nozzle-substrate distance on the optical band gap of ZnO samples

The optical band gap energy's values of the undoped and doped zinc oxide (Zn: Cr) thin films were determined using the optical process. The variation of the optical gap of films with different percentage of doping is reported in figure III.8. The band gap values found in this work are close to those reported in the literature [59].
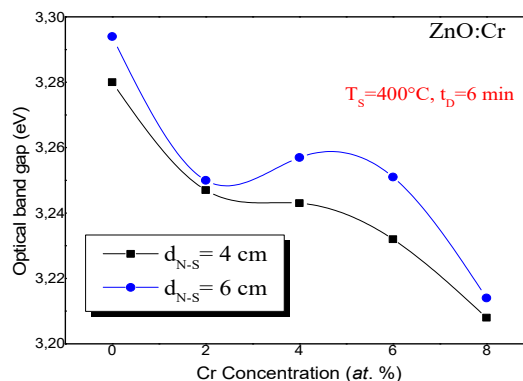
Figure III.8. Variation of optical band gap of ZnO with the percentage of Cr prepared at two different nozzle-substrate distances.

Note that the optical band gap decreases with increasing of the percentage of doping at both distances where their value range from 3.28 eV to 3.205 eV and from 3.295 eV to3.21 eV for 4 cm and 6 cm, respectively. It may be due to the next reasons [13,58,62]:

❖ When the number of particles is increased in the crystal structure, the particles cannot be placed into the proper lattice positions. This can lead to the formation of crystal defects. Therefore, the decrease in the band gap values for thin films can be due to the enhancement in photon scattering because of crystal defects which, on the other hand, create lattice strain.

❖ In terms of sp–d spin exchange interaction between band electrons and the localized d electrons of the transition metal ions substituting the cations.

❖ The increase of charge carries also the increase of energy levels.

We can note that the films prepared at 6 cm has an optical band gap more than at 4 cm that may be due to:

When the nozzle removed from the source of the prepared material, the material is formed in a regular manner, giving sufficient time for preparation, and the location of the atoms in their preferred location, with the possibility of increasing the grain size and decreasing of grain boundaries, which leads to a decrease in defects, and this allows an increase in the width of the prohibition band [17].

III.6. Effect of Cr-doping and nozzle-substrate distance on the Urbach energy of ZnO samples

Figure III.9 shows the variation of the Urbach energy of ZnO with the percentage of doping by Cr prepared at two different nozzle-substrate distances.
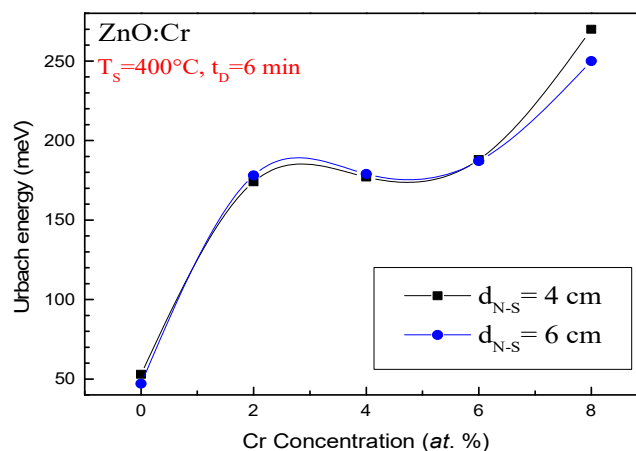
Figure III.9. Variation of the Urbach energy of ZnO with the percentage of Cr prepared at two different nozzle-substrate distances.

According to the doping percentage, we observe that the Urbach energy increase with the increasing of doping percentage from 50 meV to 270 meV and from 45 meV to 250 meV at d_{N-S} = 4 cm and d_{N-S} = 6 cm, respectively.

We observe for undoped ZnO, the E_{Urb} is smaller (47 meV) than for Cr-doped ZnO, this result is very similar to some previous works [46]. Because of the method of preparation (spay pyrolysis), this is from one hand and for the other hand the undoped ZnO films have much less impurities, defects and less disorder owing to an almost complete chemical decomposition of the precursor droplets in air or on the substrate [6,46,63,64]. By the increase of doping for both distances (4cm and 6cm), the increase of the Urbach energy observed due to the insertion of chromium atoms into the ZnO lattice thus the increases of the impurities and defects (dislocations, microstrain, grain boundaries, etc.) in the ZnO lattice [44,61,65].

From figure III.10 (a and b), we can easily observe, like several works [46,66], the inverse relationship between the variation of optical band gap and Urbach energy as a function of Cr doping concentration at two different distances [61,65].
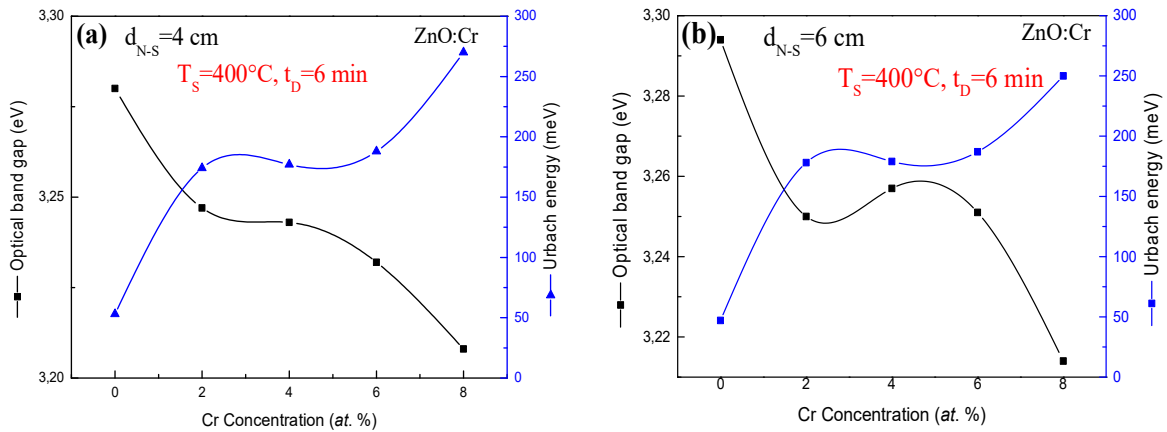
Figure III.10. The inverse relationship of E_g and E_{Urb} of ZnO thin films versus Cr doping concentration

III.7. Effect of Cr-doping and nozzle-substrate distance on the electrical conductivity of ZnO samples

The electrical characterization (conductivity, resistivity and the transport parameter) plays a very important role for the diluted magnetic semiconductor. In this study, we use the 4-probe method to determine the electrical properties.

Figure III.11 shows the variation of electrical conductivity of ZnO thin films with the percentage of doping by Cr prepared at two different nozzle-substrate distances.
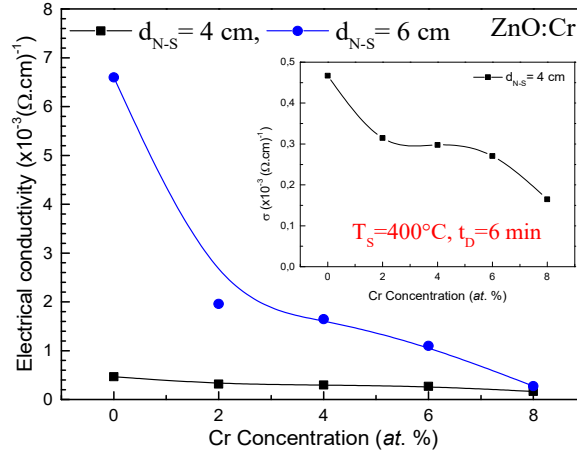
Figure III.11. Variation of the electrical conductivity of ZnO with the doping percentage by Cr prepared at two different nozzle-substrate distances.

From Figure III.11, we notice that the electrical conductivity of ZnO thin films decreases by the increasing of Cr doping percentage and by the small distance between nozzle and substrate distance. Where the conductivity values ranged between $0.47 \times 10^{-3}\ (\Omega.cm)^{-1}$ and $0.16 \times 10^{-3}\ (\Omega.cm)^{-1}$ for 4 cm and between 6.60×10^{-3} and $0.27 \times 10^{-3}\ (\Omega.cm)^{-1}$ for 6 cm.

This result may be referred to the donor defects that presented due to Cr doping that took place in zinc interstitials and oxygen vacancies in the ZnO nanoparticles host matrix, which leads to natural n-type doping [67,68]. Also, the Cr impurity in the deep level can trap the electron emitted by this defects. So in this way, it decreases the carrier density where the crystallite size decreased with the Cr concentration results in grain boundary increment which contributes to decreasing the mobility of the charge carriers and consequently, the conductivity decrease, it is well known that the electrical conductivity of semiconductors is expressed by equation III.1 [69,70]:

$$\sigma = n\ e\ \mu_n \qquad\qquad\qquad \text{III.1}$$

where:

➢ n: charge carriers concentration,

➢ e: electronic charge,

➢ μ_n: the mobility of charge carriers.

General conclusion

"ONE OF THE **BASIC RULES** OF THE UNIVERSE IS THAT **NOTHING IS PERFECT**. PERFECTION SIMPLY DOESN'T EXIST... WITHOUT IMPERFECTION, NEITHER YOU NOR I WOULD EXIST."
-STEPHEN HAWKING

HUFF POST

General conclusion

The objective of this work is to elaborate and to characterize Cr doped zinc oxide thin films deposited on glass substrate by ultrasonic spray pyrolysis technique to study the effect of doping percentage and nozzle-substrate distance on the optical and electrical properties of these films.

In this study, we used the ultrasonic spray pyrolysis because it is simple, easy to perform and does not use a vacuum. Where, the thin films prepared by this technique are a good quality and have excellent adhesion.

ZnO:Cr thin films were deposited at two different nozzle-substrate distances (4 & 6cm) from solutions of zinc acetate dihydrate ($Zn(C_2H_3O_2)_2 \cdot 2H_2O$) and chromium (III) chloride hexahydrate ($CrCl_3 \cdot 6H_2O$) dissolved in aqueous solution, with different atomic percentages of Cr (0, 2, 4, 6, and 8 *at*.%). Where, Substrate temperature, solution concentration, deposition time and flow rate were kept constant throughout the deposition process at 400 °C, 0.05 mol/l, 6 min and 60 ml/h, respectively.

The obtained samples are characterized by UV-Visible-NIR spectrophotometer and four-point probe technique to determine their optical and electrical properties. The characterization of the films lead us to the following conclusions:

With the increase in doping percentage of Cr from 0 *at*. % to 8 *at*. %, we observe that UV-Visible-NIR results showed that the optical transmittance is high in the visible range and its value ranged between 60 % and 85 % at two both nozzle-substrate distance (4 cm or 6 cm), the film thickness increases from 410 to 490 nm at 4 cm and from 355 to 485 nm at 6 cm. Also, we found that the band gap energy decrease from 3.28 eV to 3.20 eV and from 3.30 eV to 3.21 eV for 4 cm and 6 cm, respectively. We notice too that Urbach energy increases with the decrease of refractive index. Electrical conductivity of ZnO decreases by the increase in Chromium percentage from 0.47×10^{-3} to 0.16×10^{-3} $(\Omega.cm)^{-1}$ for 4 cm and from 6.60×10^{-3} to 0.27×10^{-3} $(\Omega.cm)^{-1}$ for 6 cm. These variations in this properties of deposition thin films by the increase of Cr-doping and/or the decrease in nozzle-substrate distance are interpreted by the increase in porosities, the decrease of the grain size and the increase in the donor defects that presented due to Cr doping that took place in zinc interstitials and oxygen vacancies in the ZnO matrix of the material which make it more disordered.

General conclusion

It is concluded in this work that the optical and electrical properties of ZnO:Cr thin films are varied by the variation of doping percentage and the distance between nozzle and substrate while maintaining high transparency in the visible and type of conduction, which makes it a good candidate in several fields of applications.

References

References

[1] D. Rahal & T. Zerfaoui, Elaboration of tin dioxide thin films by spray pyrolysis using different concentrations of solution and solvent, Master's Thesis, Larbi Tebessi University-Tebessa (2022).

[2] S. Redjel & N. Mekhaznia, Elaboration and characterization of tin oxide thin films deposited by spray pyrolysis, Master's Thesis, Larbi Tebessi University-Tebessa (2020).

[3] S. Guellati & C. Boussahla, Étude de l'effet de dopage par nickel et du recuit sur les propriétés des couches minces d'oxyde de cuivre, Master's Thesis, Larbi Tebessi University-Tebessa (2019).

[4] F. Ababsia & S. Fares, Élaboration et caractérisation des couches minces d'oxyde de nickel dopé au cuivre, Master's Thesis, Larbi Tebessi University-Tebessa (2018).

[5] A. Belaoura, Étude de l'effet de dopage par Sn sur les propriétés des couches minces de ZnO, Master's Thesis, Larbi Tebessi University- Tebessa (2016).

[6] L. Herissi, Élaboration et caractérisation de couches minces d'oxydes métalliques destinées à des applications optoélectroniques, Doctorate's Thesis, Larbi Ben M'hidi University-Oum El Bouaghi (2016).

[7] M. Menaa, Influence du recuit sur les propriétés optoélectroniques des couches minces de $(ZnO)_{1-x}(NiO)_x$, Master's Thesis, Larbi Tebessi University-Tebessa (2015).

[8] L. Hafsa, L. Hadjeris, L. Herissi, UV-induced photocatalytic degradation of methyl green dye by ZnO nanowires and nanorods obtained by spray pyrolysis, Nano Hybrids and Composites 36 (2022) 69-80.

[9] S. Agouram, Caractérisation de couches minces d'oxynitrures de chrome produites par pulvérisation cathodique réactive en présence d'air: influence de la vapeur d'eau contenue dans du plasma, Doctorate's Thesis, Namur University-Belgium (2003).

[10] M.M. Fahd, M. Rajab and S.M. Al-Abbas, Structural and optical characterization of Cr_2O_3 nanostructures: Evaluation of its dielectric properties 4 (2014) pp 027121-11.

[11] P. Miguel, Chromium dioxide low temperature thin film growth, structural and physical properties, Doctorate's Thesis, Lisbon University- Portugal (2008).

References

[12] J. Barnhart, Occurrences, uses, and properties of chromium, Regulatory Toxicology and pharmacology 26 (1997) 53-57.

[13] B. Maatoub & S. Fissah, Study of the optical and electrical properties of tin oxide thin films deposited by spray pyrolysis, Master's Thesis, Larbi Tebessi University-Tebessa (2022).

[14] A. Allag, S. Rahmane, A. Ouahab, H. Attouche & N. Kouidri, Optoelectronic properties of SnO_2 thin films sprayed at different deposition times, Chinese Physics 25 (2016) pp. 046801-7.

[15] A. Sari & S. Bouchrit, Elaboration et caractérisation des couches minces d'oxyde de cuivre non dopé, Master's Thesis, Larbi Tebessi University-Tebessa (2017).

[16] K. Djebbar & K. Zerroug, Elaboration par bain chimique et étude des couches minces de sulfure de cadmium (CdS) et sulfure de cuivre (CuS), Master's Thesis, Larbi Ben M'hidi University-Oum El Bouaghi (2017).

[17] L. Herissi, Élaboration par pulvérisation pyrolytique et caractérisation de couches minces semiconductrices et transparentes d'oxyde de zinc : Perfectionnement du système de dépôt, Magister's Thesis, Larbi Ben M'hidi University- Oum El Bouaghi (2008).

[18] K. Kamli, Élaboration et caractérisations physico-chimique des couches minces de sulfure d'étain par spray ultrasonique: Effet des sources d'étain, Master's Thesis, Mohamed Kheider University -Biskra (2013).

[19] S. Hariech, Élaboration et caractérisation des couches minces de sulfure de cadmium (CdS) préparées par bain chimique (CBD), Magister's Thesis, Mentouri Brothers University-Constantine (2009).

[20] S. Tosgiyuki & L. Hong, Vacuum vaporization in the system MgO-Cr_2O_3, Journal of the American Ceramic society 61 (1978) 326-329.

[21] M. Tadatsugu, I. Satoshi, M. Toshihiro & M. Youhei, Transparent Conducting ZnO thin films deposited by vacuum arc plasma evaporation, Thin Solid Films 445 (2003) 268-273.

[22] A. Hafdallah, Étude du dopage des couches minces de ZnO élaborées par spray ultrasonique, Magister's Thesis, Mentouri Brothers University-Constantine (2007).

References

[23] S. Laghrib, H.A. Adnani, D. Abdi, J.M. Pelletier, Elaboration et étude des couches minces de SnO_2 obtenu par évaporation sous vide et recuites sous oxygène, Revue des Energies Renouvelables 10 (2007) 357-366.

[24] A. Jilani, M. Shaaban, A.H. Hammad, Ch. 8: Advance deposition techniques for thin film and coating, IntechOpen (2017) 137-149.

[25] S. Kemach, Élaboration et caractérisation de couches minces de $Ni_{1-x}Zn_xO$, Master's Thesis, Larbi Tebessi University-Tebessa (2014).

[26] N. Menasraia & H. Talbi, Élaboration et caractérisation de couches minces d'oxyde de cuivre dopé par zinc, Master's Thesis, Larbi Tebessi University-Tebessa (2017).

[28] H. Benamra, L'effet de la température du substrat et de la molarité sur les propriétés des couches minces de sulfure de zinc déposées par spray ultrasonique, Magister's Thesis, Mohamed Kheider University -Biskra (2013).

[29] V. Dumitru, C. Morosanu, V. Sandu & A. Stoica, Optical and structural differences between RF and DC Al_xN_y magnetron sputtered films, Thin Solid Films 359 (2000) 17-20.

[30] T. Taouririt, L'effet du débit de la solution sur les propriétés des couches minces d'oxyde de zinc (ZnO) déposées par spray pyrolyse, Master's Thesis, Mohamed Kheider University-Biskra (2014).

[31] Y. Hamedani, P. Macha, T.J. Bunning, Ch. 10: Plasma-enhanced chemical vapor deposition: Where we are and the outlook for the future, IntechOpen (2016) 247-279.

[32] M. Daamouche, Mise ou point d'une technique d'élaboration des couches minces métalliques par voie électrochimique, Magister's Thesis, Hadj Lakhder University-Batna (2009).

[33] L. Baghriche, Élaboration et caractérisation des couches minces d'oxyde de zinc et sulfure de zinc préparées par spray ultrasonique, Doctorate's Thesis, Mentouri Brothers University-Constantine (2015).

[34] A. Hannachi, A. Segura, H.M. Meherzi, Growth of manganese sulfide (α-MnS) thin films by thermal vacuum evaporation: Structural, morphological, optical properties, Materials Chemistry and Physics 6 (2016) 326-332.

References

[35] K. Hachemi & NL. Haddar, Influence du temps de dépôts sur les propriétés des couches minces de CuO élaborées par spray pneumatique, Master's Thesis, Mouhamed Kheider University-Biskra (2020).

[36] W. Menesklou, H. Schereiner, K. Hardtl & E. Ivers, High temperature oxygen based on doped $SrTiO_3$, Sensors and Actuators B 59 (1999) 184-189.

[37] S. Berrouis & D. Bensefira, Elaboration et caractérisation de couche mince NiO:Co, Master's Thesis, Mouhamed Kheider University-Biskra (2019).

[38] N. Abdelmalek, L. Hadjeris, D. Allouane, L.Herissi, S. Rahmane & H. Moualki, Structural, optical and electrical properties of ZnO: Fe thin films grown by spray pyrolysis, Journal of New Technology and Materials 04 (2014) 47-50.

[39] A. Ferdi, A. Hafdallah, B. Harkati, L. Herissi, Effect of Zn doping on the structural and optical properties of NiO thin films deposited by spray pyrolysis technique, Functional Materials 28 (2021) 669-675.

[40] L. Herissi L. Hadjeris, M.S. Aida, J. Bougdira, Properties of (NiO)1-x(ZnO)x thin films deposited by spray pyrolysis, Thin Solid Films 605 (2016) 116-120.

[41] K. Daoudi, Élaboration et caracterisation de films minces d'oxyde d'indium dope a l'etain obtenus par voie sol-gel potentialité pour la réalisation d'électrodes sur silicium poreux, Doctorate's thesis, Claude Bernard Lyon 1 University-France (2003).

[42] N.K. Seng, M.K. Ahmad, N.S. Jasmin, N.B. Zianal, N. Nayan, S.C. Fhong, A.B. Suriani, A. Mohamed, Effect of annealing time on aluminium doped tin oxide (SnO_2) as a transparent conductive oxide, Journal of Engineering and Applied Sciences 11 (2016) 8915-8920.

[43] M. Khechba, Caractérisation de la réaction inter faciale entre une couche mince de tungstène et un substrat d'acier, Magister's Thesis, Mentouri Brothers University-Constantine (2008).

[44] A. Hafdallah, L. Herissi, N. Chergui, Z. Kebaili, M.S. Aida, N. Attaf, Structural and optical properties of ZnO thin films deposited by pyrolysis spray method: effect of Al doping, Nanotechnology Letters 2 (2018) 1-3.

[45] N. Chahmat, Traitement de l'oxyde de zinc et étude de ses propriétés physicochimiques superficielles, Doctorate's Thesis, Badji Mokhtar University-Annaba (2014).

References

[46] L. Herissi, L. Hadjeris, M.S. Aida, S. Azizi, A. Hafdallah and A. Ferdi, Ni-doped ZnO thin films deposited by pneumatic spray pyrolysis, Nano Hybrids and Composites 27 (2019) 21-29.

[47] S. Chelouche, Propriétés des fenêtres optiques ZnO: Al pour cellules solaires en couches minces à base de CIGS, Magister's Thesis, Ferhat Abbas University-Setif (2012).

[48] A. Douayar, Contribution à l'étude des propriétés structurales, optiques et électriques des couches minces de l'oxyde de zinc (ZnO) dopé (fluor, indium, aluminium et néodyme), Doctorate's Thesis, Mohammed V–Agdal University-Morocco (2013).

[49] H. Benelmadjat, Elaboration et caractérisation des composites dopés par des agrégats nanométriques de semiconducteurs, Magister's Thesis, Mentouri Brothers University-Constantine (2007).

[50] P. Amami, Structure and Spin Dynamics in Cr Doped ZnO, Master's Thesis, South Africa University (2016).

[51] O. C. Rogojanu, G. A.Sawatzky & L. H. Tjeng, Stabilizing CrO by epitaxial growth, Groningen University-Netherlands (2002).

[52] A.F. Dawood, A.L- Niaimi. & N.A. Mahmood, Effect of thickness on optical properties of (Cr_2O_3) thin films Prepared by Chemical Spray Pyrolysis Technique, Diyala Journal for Pure Sciences 12 (2016)153-161.

[53] J.Q. Brown, K. Vishwanath, G.M. Palmer & N. Ramanujam, advances in quantitative UV-Visible spectroscopy for clinical and pre-clinical application in cancer, Current Opinion in Biotechnology 20 (2009) 119-131.

[54] S.J. khmayies, R.N. Ahmad-Bitar, A study of the optical bandgap energy and Urbach tail of spray-deposited CdS:In thin films, Material Research Technology 2 (2013) 221-227.

[55] L. Herissi, L. Hadjeris, H. Moualkia, N. Abdelmalek, N Attaf, M. S. Aida, J. Bougdira, Realization and study of ZnO thin films intended for optoelectronic applications, Journal of New Technology and Materials 1 (2011) 39–43.

[56] N. Jebbari, N. Kamoun, R. Bennaceur, Effect of $SnCl_4$ concentration on $F:SnO_2$ deposited by chemical spray pyrolysis, The proceedings of International Renewable Energy Congress - (Tunisia) 2 (2010) 276-279.

References

[57] M. Mekhnache, H. Benzarouk, A. Drici, Structural linear and non-linear optical properties of Cr-doped ZnO thin film for optoelectronics applications, Materials & Research 112 (2021) 150-157.

[58] H. Aydin, C. Aydin, A.A. Al-Ghamdi, W.A. Farooq, F. Yakuphanoglu, Refractive index dispersion properties of Cr-doped ZnO thin films by Sol-gel spin coating method, Optik 127 (2016) 1879-1883.

[59] S. Yilmaz, M. Parlak, S. Ozcan, M. Altunbas, E. Bacaksiz and E. Meglynn, Structural, optical and magnetic properties of Cr doped ZnO microrods prepared by spray pyrolysis method, Applied Surface Sciences 257 (2011) 9293-9298.

[60] S. Abed, Elaboration et étude des propriétés optiques non linéaires des couches minces de ZnO dopées par nickel, fer et bismuth, Doctorate's Thesis, Mentouri Brothers University-Constantine (2012).

[61] H. Serrar, A. Bouabellou, Y. Bouachiba, A. Taabouche, A. Bouhank, Y. Bellal, H. Merabti, Effect of water and methanol solvents on the properties of CuO thin films deposited by spray pyrolysis, Thin Solid Films 686 (2019) 137-282.

[62] I. Amjid, M. Arshad, M. Taj, A. Ejaz, Structural and optical properties of Cr doped ZnO crystalline thin films deposited by reactive electron beam evaporation technique 23 (2013) 64-69.

[63] L. Hadjeris, L. Herissi, M. Benbouzid, N. Attaf, M.B. Assouar, T. Easwarakhanthan, M.S. Aida, J. Bougdira, A. Mahdjoub, Structural-optical and electrical characterization of transparent and semiconducting ZnO thin films grown by spray pyrolysis, Algerian Journal of Advanced Materials 4 (2008) 9-12.

[64] L. Hadjeris, L. Herissi, M. Assouar, T. Easwarakhanthan, J. Bougdira, N. Attaf and M S. Aida, Transparent and conducting ZnO films grown by spray pyrolysis, Semiconductor Science and Technology 24 (2009) pp. 035006-6.

[65] Z. Moussa, L. Hadjeris, L. Herissi & N. Attaf, Zn-doped iron oxide thin films prepared by spray pyrolysis technique and characterized for use as an efficient photocatalyst for methyl green organic dye, Nano Hybrids and Composites 35 (2021) 95-109.

[66] D. Beckel, A. Dubach, A.R. Studart, L.J. Gauckler, Spray pyrolysis of $La_{0.6}Sr_{0.4}Co_{0.2}Fe_{0.8}O3-\delta$ thin film cathodes, Journal of Electroceramics 16 (2006) 221-228.

References

[67] R. Ch. Prajapati, Sh. Gautam, S. Surve and Vn. Shukla, Structural, magnetic, electrical and optical studies of Cr doped nanostructured ZnO thin films for spintronics application, Materials Research Express 6 (2019) pp. 106412-10.

[68] N.M. Moussa, F.M. Ebrahim, K. Adly & M.Y. Hassaan, Chromium doped ZnO nanoparticles for energy storage, gas and humidity sensing and spin based electronic devices applications, Optical and Quantum Electronics 6 (2022) 106412 pp. 683-20.

[69] C.M. Mahajan, M.G. Takwale, Intermittent spray pyrolytic growth of nanocrystalline and highly oriented transparent conducting ZnO thin films: Effect of solution spray rate, Journal of Alloys and Compounds 584 (2014) 128-135.

Effect of Cr doping on optical and electrical properties of ZnO thin films deposited by spray pyrolysis technique

Abstract

The aim of this work is to study the effect of chromium doping and nozzle-substrate distance on the optical and electrical properties of zinc oxide thin films to ameliorate these properties, which makes it an important candidate in many technological applications such as: gas sensors, photocatalysts, and solar cells.

In this work, we have prepared chromium doped zinc oxide thin films (ZnO: Cr) at different atomic percentages (0, 2, 4, 6 and 8 *at. %*) onto glass substrates by the ultrasonic spray pyrolysis technique from aqueous solution of zinc acetate dihydrate and chromium chloride hexahydrate as precursors. Where, the experimental conditions (substrate temperature (T_S), deposition time (t_D), molarity (C) and solution flow rate (φ_S) were kept constant throughout the sedimentation process with two different distances between the spray nozzle and the substrate (d_{N-S}) for studied the effect the chromium concentration and nozzle-substrate distance on the properties of ZnO thin films deposited by spray pyrolysis. The UV-Visible spectrophotometry and four- point probe method were used to determinate the optical and electrical properties of ZnO:Cr thin films. We observed that the optical and electrical properties are influenced with the variation of chromium doping percentage and nozzle-substrate distance. The films obtained give the best physical properties (good adhesion and high optical transparency in visible range).

It should be noted that with the increase of doping percentage or the decrease of nozzle-substrate distance, the refractive index and the optical band gap decreases with increase in the Urbach energy and the film thickness, this is from one hand. On the other hand, the electrical conductivity also decreasing with the increasing of Cr percentage or as the substrate approaches the solution outlet. It should be noted that the sample that has the best electrical conductivity is the undoped ZnO that was prepared at a far distance from spray nozzle in addition to its high transparency in the visible range.

Keywords: ZnO:Cr thin films, Spray pyrolysis, Nozzle-substrate distance, Optical band gap, Urbach energy, Electrical conductivity.

Effet du dopage par Cr sur les propriétés optiques et électriques des couches minces de ZnO déposées par la technique spray pyrolyse

Résumé

L'objectif de ce travail est d'étudier l'effet du dopage au chrome et de la distance bec-substrat sur les propriétés optiques et électriques des couches minces d'oxyde de zinc afin d'améliorer ces propriétés ce qui en fait un candidat important dans de nombreuses applications technologiques telles que : capteurs de gaz, photocatalyseurs, et les cellules solaires.

Dans ce travail, nous avons préparé des couches minces d'oxyde de zinc dopé au chrome (ZnO:Cr) à différents pourcentages atomiques (0, 2, 4, 6 et 8 % $at.$) sur des substrats en verre par la technique de spray pyrolyse ultrasonique à partir d'une solution aqueuse de l'acétate de zinc déhydraté et le chlorure de chrome hexahydraté comme précurseurs. Où, les conditions expérimentales (température du substrat (T_S), temps de dépôt (t_D), molarité (C) et débit de la solution (φ_S)) ont été maintenues constantes durant tout le processus de sédimentation avec deux distances différentes entre le bec de pulvérisation et le substrat pour étudier l'effet de la concentration de chrome et de la distance bec-substrat sur les propriétés des couches minces de ZnO déposées par spray pyrolyse. La spectrophotométrie UV-Visible et la méthode de quatre points ont été utilisées pour déterminer les propriétés optiques et électriques des couches minces de ZnO:Cr. Nous avons observé que les propriétés optiques et électriques sont influencées par la variation du pourcentage de dopage en chrome et de la distance bec-substrat. Les films obtenus présentent les meilleures propriétés physiques (bonne adhérence et grande transparence optique dans le visible).

Il convient de noter qu'avec l'augmentation du pourcentage de dopage ou la diminution de la distance entre le substrat et le bec, l'indice de réfraction et le gap optique diminuent avec l'augmentation de l'énergie d'Urbach et de l'épaisseur du film, c'est d'une part. D'autre part, la conductivité électrique diminuant également avec l'augmentation du pourcentage de Cr ou que le substrat s'approche de la sortie de solution. Il convient de noter que l'échantillon qui a la meilleure conductivité électrique est le ZnO non dopé qui a été préparé à une grande distance bec-substrat en plus de sa grande transparence dans le visible.

Mots clés: Couches minces de ZnO:Cr, Spray pyrolyse, Distance bec-substrat, Gap optique, Énergie d'Urbach, Conductivité électrique.

تأثير التطعيم بالكروم على الخصائص الضوئية والكهربائية لأغشية أكسيد الزنك الرقيقة المترسبة بتقنية الرش بالإنحلال الحراري

ملخص

الهدف من هذا العمل هو دراسة تأثير التطعيم بالكروم والمسافة بين مخرج المحلول والركيزة على الخصائص الضوئية والكهربائية للأفلام الرقيقة من أكسيد الزنك لتحسين هذه الخصائص مما يجعلها مرشحا مهما في العديد من التطبيقات التكنولوجية مثل :مستشعرات الغاز، المحفزات الضوئية، وخاصة الخلايا الشمسية.

في هذا العمل، قمنا بتحضير شرائح من أكسيد الزنك المطعم بالكروم (ZnO:Cr) بنسب ذرية مختلفة (0، 2، 4، 6 و8 %) على ركائز زجاجية بواسطة تقنية الرش بالإنحلال الحراري و بإستخدام الموجات فوق الصوتية إنطلاقا من محاليل مائية من خلات الزنك ثنائي الهيدرات و كلوريد الكروم سداسي الهيدرات كسلائف. حيث تم الحفاظ على المتغيرات التجريبية (درجة حرارة الركيزة، وقت الترسيب، المولارية، ومعدل تدفق المحلول) ثابتة طوال عملية الترسيب وبمسافتين مختلفتين بين مخرج المحلول والركيزة. تم إستخدام مطيافية الأشعة الفوق بنفسجية-المرئية وطريقة المسابير الأربعة لتحديد الخصائص الضوئية والكهربائية لهذه الأفلام. لاحظنا أن الأفلام الرقيقة المتحصل عليها تمتلك خصائص فيزيائية جيدة (التصاق جيد وشفافية بصرية عالية في المدى المرئي) والتين تتأثر بإختلاف نسبة التطعيم بالكروم والمسافة بين مخرج المحلول و الركيزة.

تجدر الإشارة إلى أنه بزيادة نسبة التطعيم ونقصان المسافة بين مخرج المحلول و الركيزة، ينخفض كل من معامل الإنكسار وفجوة النطاق البصري مع زيادة العشوائية وسمك الفيلم هذا من جهة ومن جهة أخرى تتناقص الموصلية الكهربائية أيضا مع زيادة نسبة الكروم بينما تزداد إذا ازدادت المسافة بين مخرج المحلول والركيزة. وتجدر الإشارة إلى أن العينة التي لديها أفضل موصلية كهربائية هي عينة أكسيد الزنك غير المطعم التي تم تحضيرها على مسافة بعيدة من مخرج المحلول بالإضافة إلى شفافيتها العالية في النطاق المرئي.

الكلمات المفتاحية : الشرائح الرقيقة من (ZnO: Cr)، الرش بالإنحلال الحراري، المسافة بين مخرج المحلول والركيزة، عرض عصابة الطاقة، العشوائية، الناقلية الكهربائية.